

AFML-TR-64-356

**STEELS FOR SOLID-PROPELLANT  
ROCKET-MOTOR CASES**

*I. PERLMUTTER  
V. DePIERRE*

TECHNICAL REPORT AFML-TR-64-356

JANUARY 1965

AIR FORCE MATERIALS LABORATORY  
RESEARCH AND TECHNOLOGY DIVISION  
AIR FORCE SYSTEMS COMMAND  
WRIGHT-PATTERSON AIR FORCE BASE, OHIO

## NOTICES

When Government drawings, specifications, or other data are used for any purpose other than in connection with a definitely related Government procurement operation, the United States Government thereby incurs no responsibility nor any obligation whatsoever; and the fact that the Government may have formulated, furnished, or in any way supplied the said drawings, specifications, or other data, is not to be regarded by implication or otherwise as in any manner licensing the holder or any other person or corporation, or conveying any rights or permission to manufacture, use, or sell any patented invention that may in any way be related thereto.

Copies of this report should not be returned to the Research and Technology Division unless return is required by security considerations, contractual obligations, or notice on a specific document.

AFML-TR-64-356

STEELS FOR SOLID-PROPELLANT ROCKET-MOTOR CASES

I. Perlmutter  
V. DePierre

## FOREWORD

This report was written by I. Perlmutter, Chief, Physical Metallurgy Branch, Metals and Ceramics Division, Air Force Materials Laboratory and V. DePierre, Technical Manager for Metallurgical Engineering, Physical Metallurgy Branch, Metals and Ceramics Division, Air Force Materials Laboratory, Wright-Patterson Air Force Base, Ohio. The work was initiated under Project No. 7351, "Metallic Materials", Task No. 735105, "High Strength Metallic Materials"

The authors wish to express their appreciation to Mr. R. T. Ault (AFML Metallurgist), Lt. R. M. Dunco (AFML), and to all the others who contributed their advice and assistance in the preparation of this report.

This report covers a period of work conducted from July 1964 to October 1964. The manuscript was released by authors October 1964 for publication as an RTD Technical Report.

This technical report has been reviewed and is approved.



I. PERLMUTTER  
Chief, Physical Metallurgy Branch  
Metals and Ceramics Division  
Air Force Materials Laboratory

## ABSTRACT

Strength requirements for solid propellant motor cases (or chambers) are reviewed and the potential gains in performance achieved by reducing weight of inert components are discussed. It is shown that substantial improvements in strength/density ratio of booster stage material are required to effect appreciable gains in performance (velocity, payload). Weight savings are much more significant when achieved in the upper stages of a rocket system than in the booster (launch) stage. Considering the case as a pressure vessel a comparison is made between titanium alloys, aluminum alloys, a composite material (fibre glass filament winding), and alloy steels on the basis of a case optimized for resistance to internal pressure (hoop stresses) and external buckling loads. It is shown that steel would result in the heaviest chamber. However, for large boosters (above 120-inch diameter) where total weight is not as critical, the current technological advantages of heat treated alloy steel (size of necessary ingots, processing facilities, weldability in heavy sections, and cost) place this structural material in much more competitive position. Examples of technology required for large motor cases are cited. The use of special steels such as the low carbon alloy martensites, and the maraging alloys becomes mandatory for chambers of such size (260-inch diameter) that final heat treatment is not possible and the individual segments must be processed before welding.

Material reliability (performance according to design prediction) is emphasized, and related to resistance to failure by catastrophic fracture, below the design yield stress. It is demonstrated and emphasized that the higher the strength level (for a class of steels), the lower will be the reliability. Plane strain fracture toughness ( $K_{IC}$ ), the stress intensity required for initiation and propagation of a crack under maximum conditions of elastic constraint, is used as a parameter of reliability. The relations between fracture toughness, yield strength, operational stress, and geometry of crack (defect), and the use of these data in design are discussed and exemplified.

Three classes of alloy steel are comprehensively discussed in order of increasing balance between yield strength and fracture toughness. The members of Group I, the low alloy medium carbon (.35-.45C) martensitic steels, are compared with each other on the basis of the yield strength-fracture toughness relations. These steels have adequate fracture toughness at yield strength levels up to 200 ksi, in thicknesses up to 0.3 inch, and are weldable by TIG (tungsten-inert gas) welding. They are, however, susceptible to weld cracking and careful pre-heating and post-heating are required. A major disadvantage is that they must be hardened and tempered after welding. They are also susceptible to environmental cracking (delayed failure).

The second class of steels (Group II) consists of the low carbon (.25%C) alloy martensites. The metallurgical design of these alloys (9 Nickel-4 cobalt) is reviewed, and their improved balance fracture toughness and yield strength is discussed.

At a yield strength level up to 200 ksi their fracture toughness (and hence reliability) is higher than that of the medium carbon martensitic steels. They can be welded by TIG and MIG (metal-inert gas) processes after hardening without the need for final heat treatment. Thus, they are outstanding candidates for application to large cases where processing prior to welding (roll and weld) is mandatory.

The highest balance between fracture toughness and yield is attainable in the maraging steels. The physical metallurgy of these steels is reviewed and certain of their characteristics such as banding, delamination and scatter of mechanical properties are discussed.

AFML-TR-64-356

The weldability of the maraging steels of TIG, MIG and submerged arc welding is reviewed. On the basis of their combination of very high fracture toughness at high strength levels, weldability and amenability to the "roll and weld" process, these alloy steels have the highest potential for large motor cases. They are susceptible to sustained (delayed) failure, even in distilled water at high stresses.

All three classes are compared on the basis of fracture toughness-yield strength and critical flaw size-applied stress relation. The importance of future alloy steel development in the direction of improved balance between fracture toughness and yield strength for higher reliability is emphasized.

## TABLE OF CONTENTS

	PAGE
1. INTRODUCTION	1
1.1 DESIGN CONSIDERATIONS	1
1.2 COMPETITIVE MATERIALS	2
2. SUMMARY	3
3. STEELS	4
3.1 RELIABILITY AND RELIABILITY PARAMETERS	4
3.2 MEDIUM CARBON (.35 - .45%C) LOW ALLOY STEELS	6
3.2.1 WELDABILITY	8
3.3 LOW CARBON ALLOY MARTENSITES	10
3.3.1 PHYSICAL METALLURGY	10
3.3.2 PROPERTIES	11
3.3.3 WELDABILITY	12
3.4 18% NICKEL MARAGING STEELS	12
3.4.1 PHYSICAL METALLURGY	12
3.4.2 MECHANICAL PROPERTIES	14
3.4.3 BEHAVIOR	14
3.4.4 WELDABILITY	15
4. DESIGN CONSIDERATIONS	17
4.1 MATERIAL RELIABILITY COMPARISON	17
4.2 MAXIMUM STRENGTH-TO-WEIGHT VERSUS MAXIMUM RELIABILITY	17
REFERENCES	19
APPENDIX	60

## ILLUSTRATIONS

FIGURE		PAGE
1.	Typical Solid-Propellant Rocket Motor Including Case, Propellant and Nozzle	22
2.	Performance Increases from Reduction of Structural Weight of First Stage of Typical Booster.	22
3.	Weight of Cylindrical Portion of Rocket Motor Case Per Unit of Enclosed Volume Versus an Equivalent External Load Parameter (Internal Pressure = 400 psi).	23
4.	260" Diameter "Y" Ring Steel Forging	24
5.	Cross-Section of 260" Diameter "Y" Ring	24
6.	Burst Test Results for 17-7 PH Steel Tanks Tested at Room Temperature	25
7.	0.2% Yield and Ultimate Uniaxial Tensile Strength vs. Ultimate Burst Hoop Strength for 24 in. Diam. and 6.660 in. Diam. D6AC Subscale Test Vessels.	25
8.	Fracture Mode Transition	26
9.	Surface-Cracked Specimen	26
10.	Surface-Cracked Fracture Toughness Specimens (a & b 4340 and C H11)	27
11.	Flaw Shape Parameter Curves for Surface and Internal Cracks	27
12.	Range of Plane Strain Fracture Toughness Values, $K_{IC}$ , for D6A-C Steel (References 21 and 22)	28
13.	Range of Plane Strain Fracture Toughness Values, $K_{IC}$ , for 4335V Steels (Reference 23)	29
14.	Range of Plane Strain Fracture Toughness Values, $K_{IC}$ , for 4340 Steels.	30
15.	Range of Plane Strain Fracture Toughness Values, $K_{IC}$ , for H11 Steels.	31
16.	Average Plane Strain Fracture Toughness ( $K_{IC}$ ) Values for Group I Steels.	32



## ILLUSTRATIONS (CONT'D)

FIGURE		PAGE
17.	Comparison of Air, Argon and Distilled Water Environments on Delayed Failure Characteristics of 4340 and 300 M Steels at 68°F.	33
18.	Delayed Failure Characteristics of 4340, 300 M and H-11 Steels, in Distilled Water at 68°F.	33
19.	Segmented Chamber Construction	34
20.	Temperature Range of Martensite Formation in 1013 and 4315 Steels and Idealized Cooling Curves for Each of Three Specimen Thicknesses Quenched in Ice-Brine.	34
21.	Effect of Tempering Temperature on the Strength and Toughness of HP-9-4-25 Steel (Reference 31)	35
22.	Average Plane Strain Fracture Toughness ( $K_{IC}$ ) Values for Group I and Group II Steels	36
23.	Bend Tests 3/8 in. Thick x 1 in. Showing Full Cold Bend Developed With No Evidence of Cracking (Courtesy of Republic Steel Corporation).	37
24.	Iron-Nickel Equilibrium Diagram	38
25.	Effect of Titanium Content on the Yield Strength of 18 Ni (300) Maraging Steel Annealed at 1500°F and Aged at 900°F for 3 Hours.	39
26.	Representative Microstructure of 18% Ni-Co-Mo (270 ksi) 0.400" Plate Etchant: 50 ml HCl + 25 ml HNO <sub>3</sub> - 1 Cu Cl <sub>2</sub> - 15 ml H <sub>2</sub> O Magnification 500X	39
27A.	Amount of Reverted Austenite in Maraging (250) Steel vs Aging Time at Various Temperatures.	40
27B.	Electron Micrograph of Surface Replica of 18 Ni (250) Maraging Steel Overaged 10 hours at 1000°F.	41
28.	Tensile and Impact Properties of 18 Ni (250) Maraging Steel Plate at Cryogenic Temperatures 1/2 inch Plate	42
29.	Range of Plane Strain Fracture Toughness Values, $K_{IC}$ , For 18 Ni Maraging Steels (References 21, 22, 23, 25, 26 and 27)	43

## ILLUSTRATIONS (CONT'D)

FIGURE		PAGE
30.	Average Fracture Toughness ( $K_{IC}$ ) Values Versus Yield Strength (Room Temperature) for Groups I, II and III Steels.	44
31.	Segregation Observed in 18% Ni-Co Mo (270 ksi) 0.400" Plate. Magnification 500X	45
32.	Austenite and Segregation Bands in Rolled Plate of Maraging (250) Steel. Light Micrograph of Polished and Etched Longitudinal Section. X200.	45
33A.	Fracture Appearance of Smooth and Notched Tension Test Specimens of Maraging (250) Steel Showing Longitudinal "Splits" and "Internal Shear Lips"	46
33B.	Fracture Path Through Austenite Bands of Test Fracture Shown in A X200	46
34.	Orientations of Fracture Toughness Specimens Cut from 1 inch thick Plate of Maraging (250) Steel	47
35.	Laminated Maraging Plate	48
36.	Stress Corrosion Curve	49
37.	Schematic Illustration of the Different Hardening - Response Regions in 18% Nickel Maraging Steel Weldments	49
38.	Effect of Weldmetal Composition and Deposition Technique on the Net Fracture Strength in 3/4" 18Ni-7Co-5Mo Airmelted Steel	50
39.	Relative Flaw Sizes of Steels with 200 ksi Yield Strength (.2% Offset)	51
40.	Critical Flaw Size and Case Thickness Versus Yield Strength for Missiles (Internal Pressure=660 psi)	52

## TABLES

	PAGE
1. Chemical Compositions of Steels	53
2. Mechanical Properties of Group II Low Alloy Martensites	54
3. Properties of Tungsten-Inert-Gas (TIG) Arc Welded 1 inch HP 9 Ni-4Co .25C Plate Using .062 in. diameter Filler Wire of Similar Composition With Plate in Heat Treated Condition	55
4. Chemical Compositions and Average Tensile Properties of the 18 Percent Ni Maraging Steels	56
5. Properties of Welds in 18% Maraging Steel (Reference 33)	57
6. Critical Flaw Sizes and Case Thicknesses for 60-, 120- and 260-in. Diameter Steel Missiles	58
7. Mechanical Properties of Weldments	59
8. Material Properties	63

## 1. INTRODUCTION

The purpose of this report is to review the current status of steel for aerospace and related applications, in particular, for solid-propellant rocket-motor cases. While our discussion will be limited to an assessment of the current and future potential of high strength steel for this component in relation to such competitive materials such as titanium, aluminum and composites, it is hoped that it will also throw some light on problems associated with the use of wrought and welded high strength steel in other aerospace hardware.

### 1.1 DESIGN CONSIDERATIONS

Although the technology and design of rocket motors is beyond the scope of this discussion, a brief review of some elementary concepts is in order at this time. A self-explanatory sketch of a typical solid-propellant rocket motor case is shown in Figure 1. The burning of the solid-propellant grain produces a combustion pressure which is transmitted through the low modulus propellant layer to the case, and thus the latter can be considered as a thin wall internal pressure vessel. The stresses due to the internal pressure are biaxial hoop stresses in the wall and relatively localized discontinuous stresses at the junctions of the cylinder with the end closures and the skirts and of the aft closure with the nozzle ports. In addition to the internal pressure, the case is also acted upon by external inertia loads, the magnitudes and distribution of which will depend upon the factors involved in the design and mission (geometry, size, velocity, stage, and number of nozzles and so forth). These resulting external stresses are chiefly axial compressive and longitudinal bending which may induce structural instability through buckling and can interact with the internal stresses, favorably or unfavorably, depending on the stage involved. In addition, there are the high operational stresses to which the adapters, rings, skirts and other hardware attached to the casing wall are subjected. Finally, it is important to emphasize that even for a particular stage within a vehicle of a given mission profile, the stresses are functions not only of location and time but also of structural configuration and material properties.

Since the objective of a rocket system is to place a desired payload at a particular location with a given velocity, the efficiency of any stage is defined as the ratio of propellant mass before burning to the total mass (propellant plus inert components such as casing, nozzles, insulation and so forth). This ratio is called the "mass fraction", which must be achieved to as high a value as possible, particularly in the upper stages of a rocket system. Thus structural materials must be used efficiently, that is, materials must be selected to minimize the structural weight for a given propellant mass.

The present state of the art is such that a "mass fraction" of 0.9 is within current technological capability, with ten percent of the total weight being accounted for by the sum of the weight of inert parts. Thus, substantial improvements in strength to weight ratio are required to effect appreciable gains in performance. The magnitude of the potential improvement (Reference 1) is shown in Figure 2, which gives the relations between structural weight, payload and performance (design velocity) for a first stage motor in a typical launch vehicle. It will be noted that the gains in performance are significant only for decreases in structural weight of 20 to 40 percent, for payloads of the order of 2 to 4 percent of the launch weight. Such a weight reduction can be achieved, but at the expense of concomitant major problems in reliability, technology and cost. On the other hand material of higher strength-to-density ratio become more effective in improving performance when applied to upper stages rather than the launch (first stage). For upper and payload stages a pound saved in structural weight can save as much as 500 pounds of

launch weight, and furthermore only 1/500 as much material is used in the upper stages as in the lower stages (Reference 1). The cost and technological problems are of course, less severe for the smaller stages.

## 1.2 COMPETITIVE MATERIALS

The effect of material selection on the structural weight of a rocket-motor case designed to operate at a typical burning pressure of 400 psi and for certain missions, is shown in Figure 3 in which is plotted cylindrical case weight per inclosed volume against an external load parameter,  $P_{eq}/D^2$  where  $D$  = diameter of case and  $P_{eq}$  = axial compression load, equivalent to the actual combination of axial compression and pure bending (Reference 2). The derivation of this parameter and assumptions for the calculations are shown in the Appendix. The room temperature tensile properties (see Table 8) used in the calculations have been chosen to embrace the entire range from moderate strength weldable to very high strength, marginally weldable or non-weldable material. For example X7106 is the strongest weldable aluminum alloy whereas 7075 is a very strong non-weldable alloy. It will be noted that each curve consists of a straight horizontal line and a sloping segment. The former indicates that the critical stress for failure of a case is due to the internal pressure (hoop stresses), and the  $W/V$  value is independent of external loading. Beyond the intersection (transition point) of the horizontal line with the sloping line, the critical stress for failure is then due to buckling and  $W/V$  is a function of the parameter  $P_{eq}/D^2$ . The value of this parameter depends on the mission and configuration of the propulsion system. It is important to note that the titanium alloys and the composites will result in the lightest motor cases (smallest  $W/V$ , regardless of loading conditions. However, this picture is based upon the ratios of ultimate strength to density and modulus to density only. In the selection of materials there are other factors which must be considered which are at least equally important and may in certain cases offset the apparent advantages. For example, the filament winding technology results in an anisotropic product in which the orientation favorable for resisting hoop stresses is not optimum for maximum resistance to buckling. Furthermore the anisotropic nature of the composite material so complicates design analyses and manufacturing problems in the case of multi-nozzle stages that extra material must be added at the ports to allow for nozzles. Both of these considerations lower the weight advantage of composites over steel.

Titanium alloys pose major problems (particularly for large size cases greater than a 60-inch diameter) in materials cost, availability of heavy sections, and general technology (forging, heat treating, and welding). For example, consider the "Y" ring forging of maraging steel shown in Figure 4 in comparison to the current capability of the titanium alloy industry, and also the cost of material removed by machining the finished "Y" ring, a cross-section of which is shown in Figure 5. The cost of titanium alloys is much higher than that of steel. There are also current limitations on furnace sizes with stringent atmospheric controls for heat treating titanium alloys. The welding of heavy forgings and plates has not attained a satisfactory level of reliability for the high strength titanium alloys, which must be heat treated only after the welding operation. Such a sequence of operations is not feasible for ultra-large size boosters. For large cases greater than 120 inches in diameter, it becomes necessary to forge and heat treat individual segments of the cases prior to welding. Field repair by welding such as shielded arc welding will be necessary.

It is in the area of very large booster cases especially that steel enjoys a wide margin over the competitive materials. Nevertheless, these materials (titanium alloy and glass-filament windings) have made considerable inroads on the position of steel in the motor

case field particularly for smaller upper stages where technology is not a limiting factor and higher cost is justified by improved performance. For the large booster case, above 120 inches in diameter, the position of steel remains at present unchallenged.

## 2. SUMMARY

This survey has pointed out that for applications involving conditions of plane strain (maximum elastic restraint), at 200 ksi yield strength, three groups of steels, each with a different level of fracture toughness, are available. In the range 200-300 ksi yield strength, the choice is limited to two groups.

As the carbon increases, yield strength capacity increases but fracture toughness decreases. Silicon and the carbide formers lower the fracture toughness but nickel usually tends to increase fracture toughness and solid solution strength. Optimum balanced compositions, based on combinations of carbon and alloying elements in relation to their effect on strength, toughness and tempering response of the martensite is represented by the low carbon alloy martensites. This group is typified by the 9-4-25 alloy, which has higher fracture toughness at the 200 ksi level, than the structural .35/.45C martensitic steels. Future research on the low carbon alloy martensites should be aimed at achieving a uniformly fine lower bainite in such steels which may further improve their fracture toughness (Reference 37).

The traditional .35/.45C martensitic steels offer the lowest level of fracture toughness. However recent investigations (Reference 22) have indicated that if a lower-bainite, free from martensite, is attained, high fracture toughness can be achieved at a yield strength of 250 ksi in a .45 carbon alloy steel. Pascover et al. Reference 22 reports exceptionally high values in the alloy steel containing 9 Nickel-4 cobalt-.45 carbon.

Future research on alloy compositions to achieve a 100 percent lower bainite could be fruitful. However applications based on the austempering treatment would be very specialized.

The highest level of toughness, is exhibited by the maraging steels. They derive their high yield strength from precipitation hardening reactions and not from carbon. The efficient use of these steels is somewhat limited by the reduced fracture toughness in the weld, and the scatter of the toughness properties. The scatter undoubtedly reflects the influence of processing variables on the kinetics, morphology and distribution of the precipitates. The aging response of the weld metal probably is a controlling factor in its toughness characteristics. Therefore future research should concentrate on the effects of the processing variables and more intensive welding studies.

Because of certain technological advantages, steel currently is the undisputed leading candidate for first (booster) stage motor cases. However, competition by titanium and filament wound cases requires that improvements in steel be made or it will be replaced, as it has in a number of instances. The steel metallurgist has his job cut out for him.

### 3. STEELS

#### 3.1 RELIABILITY AND RELIABILITY PARAMETERS

The selection of a high strength steel for motor case application is dependent on three main interrelated properties:

- a. Yield Strength Capability
- b. Reliability
- c. Fabricability (particularly Weldability)

These properties are interdependent and the final selection of the steel is based on optimum combination of all three. The significance of the tensile properties has already been indicated in connection with design considerations and will not be discussed further. Fabricability will be considered in the discussion of individual steels. The subject of reliability has not hitherto been defined and some treatment of the subject is necessary.

Material reliability can be defined as the ability of a material to reproducibly perform according to design expectation. For structural steels the definition implies that the material should fail by gross yielding rather than by catastrophic fracture below the design yield stress. The brittle fracture of high strength components has been attributed to small flaws incurred in fabrication. These flaws act as stress raisers which produce premature failure at applied stress levels below the design limit. If high strength steels have no flaws or if sufficient toughness exists so that flaws do not propagate as cracks, reliable material performance can be predicted from the strength parameters obtained in a smooth tensile test. In practice, however, all flaws cannot be removed and service tests on components made from materials heat treated to very high strengths indicate that a large scatter in failure behavior will occur. Figure 6 (Reference 4) illustrates this point for thin-wall pressure vessels, namely, that at the higher strength levels the probability of failures increases and hence reliability decreases. Figure 7 (Reference 5) also shows the same effect at higher stress levels in another type of steel. It is obvious that strength alone cannot be the criterion for steel performance. The probability for premature (brittle fracture) failure and therefore the reliability, as indicated in Figures 6 and 7, can be related to the strength of a material in the presence of a sharp notch. The determination of the behavior of a material in the presence of a sharp notch (crack-like defect) is usually evaluated by the conventional notch tensile or notched impact tests. However the results are usually a function of the geometry of the specimen, and have value only for screening and very limited application to design.

The most significant and quantitatively useful parameter of material reliability is based upon concepts of fracture mechanics (References 6 and 7). From elastic stress analysis, the magnitude of the stress intensity ( $K$ ) surrounding the initial crack (the defect) can be calculated. At the instant of failure (when the crack becomes unstable) the stress intensity is designated as  $K_c$  which is termed the fracture toughness. The fracture toughness ( $K_c$ ) is related to the energy necessary for crack propagation under conditions of plane stress. As the thickness of the specimen containing the crack is increased, the degree of elastic restraint increases and the value of  $K_c$ , the fracture toughness, decreases to a constant value,  $K_{IC}$ . Figure 8 shows the transition and indicates schematically the change from shear mode (high energy) to normal mode (low energy). The

value  $K_{IC}$  therefore represents the stress intensity which will initiate and catastrophically propagate a crack under conditions of maximum elastic restraint. The value  $K_{IC}$ , the fracture toughness under plane strain conditions, represents a material parameter which is independent of component geometry.

The measurement of  $K_{IC}$  can be accomplished by a variety of techniques, the details (Reference 8) of which are beyond the scope of this discussion. One method illustrated in Figure 9 is to initiate a partial surface crack (defect) by means of a sharp tool indentation, an elox-type electrical discharge or a drilled hole, and then developing a crack by bending fatigue. The specimen is then pulled in tension. Figure 10 depicts typical fractured surfaces, showing slow fatigue pre-crack and relative proportions of normal and shear fracture.

The value of  $K_{IC}$  is calculated as follows:

$$K_{IC} = \frac{1.1 \sigma \sqrt{\pi} a}{\left[ 2 - .212 \left( \frac{\sigma}{\sigma_{ys}} \right)^2 \right]^{1/2}} \quad \text{(For Surface-Flawed Specimens)} \quad (1)$$

Where  $K_{IC}$  = plane strain stress-intensity factor, ksi  $\sqrt{\text{in.}}$

$\sigma$  = gross area fracture stress (ksi)

$\sigma_{ys}$  = .2% offset yield strength (ksi)

$$\phi = \int_0^{\frac{\pi}{2}} \left[ 1 - \frac{(c^2 - a^2)}{c^2} \sin^2 \theta \right]^{1/2} d\theta$$

$a$  = Depth of elliptical surface flaw (inches)

$2c$  = Length of elliptical surface flaw (inches)

$\theta$  = Integration variable

$\phi$  depends on flaw dimensions,  $a$  and  $c$ , only.

$$\left[ 2 - .212 \left( \frac{\sigma}{\sigma_{ys}} \right)^2 \right] = Q, \text{ Flaw shape parameter}$$

Substituting  $Q$  in equation (1) gives

$$K_{IC} = 1.1 \sigma \left( \frac{a}{Q} \right)^{1/2} \sqrt{\pi} \quad (2)$$

$\frac{a}{Q}$  is called "Relative Flaw Size" a quantitative relative value of defect size producing catastrophic failure in a given material under an applied stress. The flaw shape parameter,  $Q$ , is shown graphically as a function of crack dimensions in Figure 11 and in this form is very useful as will be shown.



In the subsequent discussion,  $K_{IC}$ , the plane strain fracture toughness, our parameter of material reliability will be used to compare the different steels. The applicability of this concept to design considerations is illustrated in the following example.

Suppose after heat treatment and machining, cracks having a depth ( $a$ ) of 0.030 inch and a length ( $2c$ ) of 0.250 inch may exist in the finished product due to limitations of non-destructive testing techniques. If the operating stress ( $\sigma$ ) is 200 ksi and H11 steel heat-treated to 220 ksi yield strength is selected for this application, the minimum fracture toughness ( $K_{IC}$ ) required to prevent catastrophic failure can be calculated from Equation 2 with  $\sigma = 200$  ksi,  $a = .030$  inch and " $Q$ " (obtained from Figure 11 for  $a/2c = .12$  and  $\sigma/\sigma_{YS} = 0.91$ ) equal to 0.90. The calculated fracture toughness ( $K_{IC}$ ) is 68 ksi  $\sqrt{\text{in.}}$  for the assumed conditions. Reported values of  $K_{IC}$  for H11 steel, heat-treated to this yield strength level, range from 25 to 60 ksi  $\sqrt{\text{in.}}$  with an average value of about 45 ksi  $\sqrt{\text{in.}}$ . Therefore either the applied stress must be reduced (at the same flaw size) or, if this is not possible, a steel of higher fracture toughness must be selected. The range of commercially available steels to meet this requirement is the subject of the remainder of this paper. Discussion is limited to those steels having a minimum capability of 150 ksi yield strength. Their chemical compositions are given in Table 1, from which it is seen that they fall into approximately three groups:

- I. Medium Carbon Low Alloy Steels
- II. Low Carbon Low Alloy Steels
- III. Maraging Steels

### 3.2 MEDIUM CARBON (.35-.45%C) LOW ALLOY STEELS

Because of their carbon content and high hardenability the medium carbon low alloy steels have a high yield strength capability, readily attainable by quenching and tempering. Chemical compositions of these steels are listed in Table 1; since conventional tensile properties of these steels are rather well known, they will not be repeated here. Parts made of these steels are welded in the annealed condition, heated to the 1550°-1650°F range, quenched in oil, water, or molten salt (depending on wall thickness) and tempered to obtain the desired yield strength level.

Fracture Toughness - Yield strength relations for each of the steels of this group (H11, 4335V, 4340, and D6A-C) are presented in Figures 12-15, in which are plotted, as function of yield strength, all the values of  $K_{IC}$  reported in the literature. The average values of  $K_{IC}$  in these figures are also plotted for comparison in Figure 16.

It will be noted that for all steels the fracture toughness ( $K_{IC}$ ) remains at low level at high yield strength values but rapidly increases in a critical yield strength range that is characteristic of the particular steel composition. It is important to emphasize at this point that  $K_{IC}$  is the stress intensity factor under conditions of plane strain (maximum restraint). In thin sections, however, say sheet less than 0.080 inch thick, plane stress conditions (much less restraint) prevail and the fracture toughness parameter under these conditions,  $K_c$ , the stress intensity for catastrophic crack growth, will be much higher. For example at 200 ksi yield strength the steel D6A-C (Figure 12) has an average

$K_{IC}$  (plane strain fracture toughness) of 75 ksi  $\sqrt{\text{in.}}$ . However in a section of about 0.080 inch thick (plane stress), the stress intensity factor,  $K_c$ , (plane stress fracture toughness) would be about 200 ksi  $\sqrt{\text{in.}}$ , and would maintain a value well about 75 ksi  $\sqrt{\text{in.}}$  in sections up to .25-.30 inch thick. This steel at the 180-210 ksi yield strength level is widely used for motor-cases. Extensive investigations have shown that in section thicknesses up to .25 inch, both D6A-C and 4335V alloys can be used at a nominal 180 ksi yield strength level with adequate parent metal and weldment fracture toughness. For thick-wall sections (about 0.5 in.), these materials must be used at yield strength levels not in excess of the 160-180 ksi range to assure adequate plane-strain fracture toughness. In general it appears that tempering these steels to yield strength levels of less than 220 ksi would be the only way to effect an optimum compromise between fracture toughness (reliability) and yield strength.

At present vacuum melted materials are preferred over the air-melted type. Currently the U. S. steel industry is making considerable effort to approach the vacuum technology by air-melting combined with special treatments, principally vacuum ladle degassification. It can be said, however, that at present the quality (non-metallic inclusions, sulphur-phosphorus content, and so forth) of the latter is not comparable to that of vacuum melting, but is appreciably superior to that of air-melting (Reference 9).

The large scatter in the data of Figures 12-15 is due to several factors. Several of the steels were air-melted and others vacuum-melted. Furthermore, it has been demonstrated (Reference 10) that sulphur and phosphorus play an important role in fracture toughness. Perhaps the most significant factor is the test technique. It is certain that there will be appreciable differences in  $K_{IC}$  values for a given material tested with either pre-cracked center-notch, surface cracked, notched round bar or notched bend test specimens. Another major influence on scatter of fracture toughness is due to the fact that these medium carbon, low alloy steels are particularly susceptible to delayed failure in aqueous environments (Reference 11). This is illustrated in Figures 17 and 18 which depict the results of environmental tensile tests on center-notched, pre-cracked specimens. These figures are self-explanatory and lead to the following conclusions:

1. Moisture content of test environment reduces both the failure stress (at constant test time) and the failure time (at constant applied stress) of notched specimens (see Figure 17).

2. On material of the same composition the deleterious effects of environmental moisture on notch tensile strengths are more pronounced at high yield strength levels (206 ksi) than at lower yield strengths (186 ksi) (see Figure 18).

3. At the same yield strength level delayed failure characteristics due to environmental moisture is a function of the test material composition (see Figure 18). The effects of environmental moisture on fracture toughness of steels assume great importance in the hydrostatic proof testing of motor-case where water is utilized as the pressure medium and also in high humidity service conditions. It is interesting that less than one grain of moisture per cubic foot of gas could induce delayed failure in these steels (Reference 11). Test results to define the embrittlement mechanism indicate that hydrogen produced by corrosion is the primary cause of the embrittlement.

Figure 16 presents a summary of the average  $K_{IC}$  - yield strength relations for the

Group I steels. It is seen that H11 has the lowest fracture toughness and D6A-C the highest. Referring now to our example (paragraph 3.1) where at the design yield strength of 220 ksi a fracture toughness of 68 ksi  $\sqrt{\text{in.}}$  was required, it will be recalled that the fracture toughness (45 ksi  $\sqrt{\text{in.}}$ ) of H11 was inadequate. Our study of the Group I class has brought out only one candidate, namely D6A-C, with an average fracture toughness value of 75 ksi  $\sqrt{\text{in.}}$  at the 220 ksi yield strength level. However the designer must take into account the entire D6A-C scatter band (see Figure 12) which indicates a range of about 50 to 80 ksi  $\sqrt{\text{in.}}$  for 220 ksi yield strength. This does not meet reliability requirements and the search must continue for more reliable materials.

Considerable research on the relations between microstructure and fracture toughness of these steels (Medium Carbon Low Alloy Steels) indicates that in the very high strength, low fracture toughness range, the microstructure of the associated martensite is characterized by high dislocation density, many micro-twins and a film of epsilon carbide surrounding the martensite and twin boundaries. The films act as preferred paths for crack propagation through the structure. For good fracture toughness the net work must be eliminated, by spheroidization, and the lattice defects by a recovery treatment. These desirable microstructural changes cannot to date be achieved (Reference 10) by alloying elements such as silicon which raise the resistance to tempering. At present it must be concluded that carbon-strengthening alone has limited potential in the development of very high strength steels (greater than 200 ksi yield strength with good toughness).

There is good evidence that the balance between strength and toughness of Group I steels can be appreciably improved by special processes such as ausforming or isothermal transformation to bainite. However for motor cases of appreciable size the necessary processing and heat treatment to accomplish the desired microstructure and properties would involve serious economical and technological difficulties. One could, of course, lower the carbon content to achieve higher toughness and thereby maximize reliability but for airborne structures this involves maximization of the weight problem.

### 3.2.1 WELDABILITY

The factors which favor the yield strength capability in these Group I steels, namely carbon and alloy contents, have the opposite effect on reliability, particularly as related to the properties of welded joints. However, for smaller cases, say 65 inches in diameter, welding of Group I steels (such as D6A-C and 4335V used in 180-200 ksi yield strength range) has not been a limiting factor and reliability has been adequate. The cylindrical sections of such components are first formed by shear-spinning or machining from forgings, thus eliminating the necessity for the more highly critical longitudinal welds, and then these sections are joined to end closures by circumferential welding. For larger cases, say 120 inches and over in diameter, where shear spinning is not feasible, longitudinal welds are necessary. However up to the yield strength range 180-200 ksi, the problems are still of manageable proportions, even though the longitudinal welds must contend with the biaxial stresses of the pressure vessels. For cases over 120 inches in diameter the limitations of this type of steel even for lower yield strength levels will now become apparent. In sizes up to 120 inches in diameter, the assembly is heat-treated after welding by quenching and tempering. The fracture toughness of the weld metal for D6A-C and 4335V, after this sequence, is satisfactory relative to that of the parent metal. Typical values of weld metal toughness are 91 ksi  $\sqrt{\text{in.}}$  for 4335V and 74 ksi  $\sqrt{\text{in.}}$  for D6A-C, compared to base metal values of 91 and 90 respectively at approximately the same yield strength range. However, for cases of the order of 260 inches in diameter where final heat treatment of the assembly is not possible, consideration must be given

to a processing technique in which individual sections and segments (Reference 12) are welded after heat-treatment (see Figure 19 in which welding joints are clearly indicated). For such an application (welding after heat treatment) the strength and toughness in the weld area must approach that of the parent metal. Even in thin sections (less than 0.15 inch) and under the most optimized conditions of welding, the D6A-C welded joint is marginal in fracture toughness and therefore unsuitable for application without a final heat treatment. Welded joints of the steel 4335V, while adequate in the as welded condition in thicknesses up to 0.22 inch, falls far short of the necessary fracture toughness value in thicknesses of 0.50 inch. In heat treated plus welded condition 4335V has a fracture toughness,  $K_{IC}$ , less than 1/2 of the parent metal toughness. Since these are the toughest of the Group I steels (Medium-Carbon .35 - .45% Carbon Low Alloy Steels), it is apparent that for very large motor cases, requiring hardening before welding, this class is generally unsuitable.

At the present time, practically all the welding of Group I steel motor cases is carried out automatically by the tungsten inert gas (TIG) process (Reference 13) with the addition of filler metal. Although welding speed and deposition rate for this technique are considerably lower than for metal inert gas (MIG) or submerged arc processes and more expensive, it is preferred for thin sections (.080 to 0.30 inch). Experience to date has indicated that TIG welding results in greater freedom from porosity and higher weldment strength and fracture toughness values than produced by other welding techniques (such as MIG or submerged arc) and is not likely to be replaced by them for welding motor cases of Group I steels. Welding efficiency (weld metal yield strength percentage of parent metal yield strength) greater than 95 percent is readily obtained with TIG welding.

Since the fraction of filler metal in the weld may be as low as 9 percent and seldom exceeds 25 percent (depending on thickness and geometry of V groove and spacing and so forth), there is a wide range of selection of filler metals for Group I steels. (Reference 13) In general the practice has been to match the chemistry of the base metal with that of the filler rod for uniformity in response to heat treatment. In selection of filler rod some consideration should be given to whether the weld is longitudinal or girth type, since in the motor-case (pressure vessel) the walls are subject to a biaxial stress field. In the girth weld, the capacity for plastic strain is more important since the stresses in the weld are lower than the maximum design stress and the weld must strain to the same extent as the base metal during pressurizing. The selection of a filler rod by compromising in favor of higher plasticity and lower strength is called "undermatching". On the other hand, the longitudinal weld must have the same or better yield strength capacity as the parent metal if it is not to be a critical area for failure. However, it must have sufficient fracture toughness to cope with possible defects. In general the practice has been to use filler metals of alloy steels similar to the base metal or modifications of lower carbon. A typical filler rod composition for both girth and longitudinal welds of D6A-C steel motor-cases is the alloy steel 17-22AS (0.26/0.32C, 1.0Cr, 0.5 Mo, 0.25V). Finally of major importance in filler metal chemistry is the necessity to maintain the sulphur and phosphorous levels to values below 0.015 percent, as their presence promotes weld metal cracking by the formation of interdendritic low melting point eutectics.

The welded motor case assembly must be delivered to the heat treating furnace free from cracks incurred either in the welding operation or during handling and manipulation of the "as welded" product. To achieve this desirable state of affairs in the Group I steels, it is necessary to control the entire thermal cycle experienced by the steel, so that the austenite decomposition product is bainite rather than martensite. These operations are called "pre-heating" and "post-heating". The TTT diagrams for these steels

imply that, in general, preheat, interpass and hold (30 minutes after weld) temperatures of 600 to 700°F are necessary to achieve an all bainitic structure. Unfortunately at this temperature range the carefully cleaned surfaces oxidize and it is believed that this condition is associated with porosity in the weld. Furthermore such high temperatures cause considerable discomfort to the welding operator. Therefore the majority of fabricators have compromised at 300° to 450°F for preheat, interpass and hold temperatures. This has been quite successful presumably because the structure of mixed bainite and partially tempered martensite attainable by this thermal cycle confers on the steel sufficient ductility to minimize crack formation.

In summary the medium carbon, low alloy steels (Group I) are very useful for moderate size motor-cases. At yield strength levels of 180 to 200 ksi and in sections up to 0.3 inch, their fracture toughness is adequate, they can be welded by conventional methods, and their cost is moderate. On the other hand at higher yield strength levels above 200 ksi and in heavier sections, their fracture toughness is insufficient for reliability and they are susceptible to weld cracking and require careful pre-heating and post-heating. Finally, the necessity for final quenching and tempering precludes them from application to large cases and to field-weld repair.

With respect to the future potential of steel application in the motor case field, a number of questions now present themselves.

(1) What can be done about achieving a steel with higher fracture toughness than is indicated in Figure 16 at the yield strength range of 180 to 200 ksi?

(2) Can one achieve very high reliability (high fracture toughness) at a yield strength level of 150 ksi, other than by tempering the Group I steels (with their weld crack problems) down to this yield strength?

(3) What are the possibilities for a steel with adequate fracture toughness at a yield strength of approximately 250 ksi?

(4) Finally, what steel is available for fabrication of motor-cases so large that austenitizing and quenching of the complete structure are not possible?

There are two very promising approaches to these problems, and current activity in evaluating their potential and limitations is at a high level. They will now be discussed.

### 3.3 LOW CARBON ALLOY MARTENSITES

#### 3.3.1 PHYSICAL METALLURGY

It has been known for some time (Reference 14) that freshly quenched low carbon (less than .25%) martensite is not untempered and brittle as is the case with the higher carbon steels but rather is a tempered and relatively tough product. There are two reasons for this circumstance, namely that the low carbon quenched martensite is actually tempered during quenching and is free from epsilon carbide. This is explained in Figure 20 from the work of Aborn (Reference 14) in which are superimposed three continuous cooling curves on a diagram showing  $M_s$  and  $M_f$  values for SAE 1013 and 4315 steels. The 1013 is a plain carbon steel (0.13%C) and 4315 is a nickel-chromium-molybdenum low carbon alloy steel (0.15%C). Even though at this rapid cooling rate the only transformation product in all cases was martensite, it is important to note that the hardness at the center

of the thickest section in the SAE 4315 steel was nearly 40 VPN less than in the thin section. The softening effect caused by the sojourn in the range 750°F and 610°F ( $M_s$  and  $M_f$  for 4315) is called "Q" tempering and the tempered products have truly unique and remarkable balance between toughness and strength which can be further improved by tempering even as low as 212°F. This self-tempered low carbon epsilon-free martensite may now be alloyed for additional toughness, hardenability, strength and resistance to tempering. Out of this concept has come a series of low alloy, low carbon (less than .25% carbon) steels of moderate strength up to 200 ksi yield strength with high toughness and weldability in the as quenched or welded condition. In general these steels contain up to 9 percent nickel (for toughness and solid solution strengthening), 1-2 percent chromium (for hardenability), with vanadium and molybdenum up to 0.50 percent for resistance to tempering. An important contribution by the Republic Steel Corporation was the addition of 4 percent cobalt to the well-known tough 9 percent nickel steels to avoid the retained austenite favored by the higher carbon content necessary for high yield strength capability. The addition of 4 percent cobalt provides the additional beneficial effect of raising both  $M_s$  and  $M_f$ , thereby further promoting the self-tempering ("Q" tempering) effect.

### 3.3.2 PROPERTIES

The chemical compositions of certain of these steels are shown in Table 1, Group II. Mechanical properties of HP-9-4-25 steel as a function of heat treatment are shown in Figure 21 (Reference 15). Attention is called to the high yield strength level maintained up to 1000°F tempering temperature and particularly the good notch toughness even at the very low tempering temperature. Additional data on these and other members (USS 150 and HP 150) of Group II are given in Table 2.

The plane strain fracture toughness-yield strength relationship for low carbon alloy martensites is given in Figure 22 in which a comparison is made with average fracture toughness curves of Group I steels. It will be noted from Figure 22 and Table 2 that steels HP 150, and USS 150 are characterized by very high fracture toughness. It might be argued from Figure 22 that a comparable level of fracture toughness could be achieved in the Group I steels by tempering down to the same yield strength of approximately 150 ksi. However, it must be remembered that the latter must be heat treated after welding, and the higher carbon means greater propensity for weld cracking. On the other hand individual component segments of USS 150 and HP 150 steels can be forged, water-quenched, tempered to 1100°F, and then welded without further treatment. For this reason they have been proposed for submarine hulls, and motor cases too large for heat treatment. In spite of their reliability ( $K_{IC} = 155 \text{ ksi } \sqrt{\text{in.}}$ ) and the simplicity of their processing schedule, their strength is considered by some to be marginal for booster cases.

By increasing the nickel content to approximately 9 percent and maintaining a carbon level of 0.25 percent, the yield strength level of the low carbon alloy martensites can be increased to 200 ksi while still retaining a very high level of fracture toughness. Thus, the alloy HP-9-4-25 with moderate amounts of carbide forming elements for resistance to tempering (see Table 1, Group II) has, at a yield strength of 200 ksi, a much higher fracture toughness than steels of Group I and is weldable. Since it is a low carbon martensite, it needs only at most a localized post-heating operation after welding. This alloy steel which is water-quenched from 1500°F and tempered up to 1000°F is considered to have very high potential for a large motor case which can be fabricated by welding the assembly of heat treated segments (Figure 19).



### 3.3.3 WELDABILITY (Reference 14)

The 9-4-25 low carbon alloy martensites have been welded as 1-inch plates in the fully heat treated condition with low preheats and interpass temperatures by the tungsten-inert-gas (TIG) process. Using filler wires of compositions similar to those of the base metal, weldments with mechanical properties listed in Table 2 were achieved (Reference 15). Data in the table indicate better than 90 percent weld joint efficiency (yield and tensile strength) with Charpy V-Notch impact values at  $-80^{\circ}\text{F}$  of 31-37 ft-lbs in the weld metal. The TIG welds were free from cracks in the weld and heat-affected zone when welded under conditions of high restraint. Samples  $3/8''$  thick and 1" wide, cut from welded 1 inch plate, exhibit sufficient ductility to be bent around a 2T mandrel (Figure 23).

Although the TIG process produced HP-9-4-25 weldments with good quality and high reliability (as indicated by high  $K_{IC}$  fracture toughness values, 117-138 ksi  $\sqrt{\text{in.}}$  in Table 3), this method is slow (metal deposit rates low) and not economical for the length of weld required for large motor-cases (see Figure 19). Therefore special techniques for using the metal-inert-gas (MIG) and submerged arc welding processes are currently being developed to combine high reliability with speed and economy in welding. The use of AC-MIG welding has eliminated the magnetic field effects in DC-MIG welding which produce severe unsoundness in weld deposits. The AC-MIG weldability is so new that only a limited amount of weld data is available. In  $1/2$ -inch plates AC-MIG procedures, using filler metal of base metal composition, produced weld metal with Charpy V-Notch impact values of 27-30 ft-lbs at room temperature and 23-24 ft-lbs at  $-80^{\circ}\text{F}$ . These results have been encouraging and welding evaluation is being extended to 1-inch and 2-inch plates.

With respect to the 150 ksi class of Group II steels progress in welding (Reference 16) by the MIG process has been very successful. At a yield strength of 145-150 ksi, MIG welds have been achieved with 153 ksi yield strength, 49 ft-lbs (Charpy V-Notch  $0^{\circ}\text{F}$ ), and 125 ksi  $\sqrt{\text{in.}}$  fracture toughness. These properties have been achieved on plates 1-inch and 2-inch thick MIG welded without post heat.

## 3.4 EIGHTEEN PERCENT NICKEL MARAGING STEELS

### 3.4.1 PHYSICAL METALLURGY

The maraging steels are a class of low carbon (0.02%C) iron-nickel alloy base alloys with hardening additions of molybdenum, cobalt, titanium, and aluminum, announced in 1959 by the International Nickel Company. Although there are several types, depending essentially on nickel content, our discussion will be limited to those which are currently the most important technologically, namely those containing 18 percent nickel.

Under equilibrium conditions an iron base alloy with 18 percent nickel is completely austenitic (Gamma) at a minimum temperature of  $1180^{\circ}\text{F}$  (Figure 24). With additions of hardening elements this temperature is raised to  $1350^{\circ}\text{F}$ , and for the attainment of an all austenitic matrix, with all precipitates dissolved and relief of internal micro-stresses, a temperature of about  $1500^{\circ}\text{F}$  is required. This is termed, in practice, the annealing temperature. Upon cooling the binary Fe-18 percent nickel alloy from  $1500^{\circ}\text{F}$  the transformation to the equilibrium alpha ferrite is depressed to a sufficiently low temperature, such that diffusion rates are very slow and a reversible martensitic diffusionless shear type of transformation occurs. Particularly abnormal for iron base alloys is the reversibility of the martensitic transformation, which also takes place by a diffusionless shear process and has several important implications in the fabrication of the maraging steels.

With a minimum of 18 percent nickel the formation of martensite is assured regardless of cooling rate. The presence of substantial amounts of hardening agents such as cobalt, molybdenum, titanium, and aluminum do not affect the martensitic reaction but merely change the  $M_s$  from 550°F for the binary alloy to 310°F for the maraging alloy. The  $M_f$  for the latter is about 210°F.

The as-quenched iron-nickel martensite is a most unique product, and it is interesting to compare it with that resulting from the hardening of steel. Since there are no diffusion controlled phases resulting from the austenite transformation of the maraging alloys, regardless of cooling rate, the concept of hardenability and section size (basic to steel), are not applicable to these alloys. Also inapplicable is the principle of tempering, since other phases do not form on reheating the iron-nickel martensite (as the formation of carbides in hardened steel). The structure of the iron-nickel martensite and that of the maraging alloy are both body-centered cubic, and quite ductile, whereas freshly quenched steel (carbon content greater than 0.30%) is body-centered tetragonal and brittle. The strength of "as quenched" maraging steel is not appreciably influenced by the hardening agents (Co, Mo, Ti, Al) but rather by the 0.02 carbon, addition of which raises the yield strength of the iron-nickel martensite from 72 ksi to about 95 ksi.

When the unstable martensite of the "as-quenched" maraging alloy is reheated to the range 750 - 950°F, the temperature is still too low for appreciable reversion to austenite, but precipitation occurs, and the strength increases markedly. The degree of strengthening depends on the content of hardeners, chiefly molybdenum and titanium, and three grades of 18 percent nickel maraging steel are recognized commercially (see Table 4). An empirical formula (Reference 17) relating the strength to composition has been proposed empirically (for a 900°F aging treatment after 1500°F annealing), as follows:

Yield strength (ksi) =  $15.1 + 9.1 (\%Co) + 28.3 (\%Mo) + 80.1 (\%Ti)$ . There is however, considerable scatter, by as much as 35ksi. This indicates that response to aging varies from heat to heat, and undoubtedly also reflects the effects of processing variables. The degree of scatter is illustrated in Figure 25.

The mechanism of the age-hardening reaction has not been completely established. The compounds  $Ni_3Mo$  and probably  $Ni_3Ti$  have been identified but in the aged product the role of short-range ordering in the martensitic matrix has not yet been excluded as a factor in the hardening effect. The microstructure of the heat treated alloy is shown in Figure 26.

At the upper limit of the aging temperature range, reversion to austenite by the shear transformation begins in the martensite. At 1000°F, 3 percent austenite was observed after heating for 5 minutes, 6 percent austenite after 30 minutes, and after 1 hour at 1200°F, 50 percent austenite. The kinetics of the reversion and stabilization reactions are shown in Figure 27A which indicates that for each aging temperature there is a time beyond which reversion to austenite proceeds quite rapidly. There are at least three important implications of the reversion phenomenon, from a practical point of view.

1. The temperature range for aging is narrowed considerably, thus curtailing flexibility in control of properties (as in steel). For example in Figure 27A after 3 hours at 900°F (the usual aging treatment) about 2 percent retained austenite is observed. Thus austenite reversion and stabilization is a form of overaging illustrated in Figure 27B.



2. The refinement of grain size, attainable in steel by heating into the austenitic range, is not possible in the maraging alloys when the austenite is achieved by reversion. Plastic deformation is necessary, otherwise the grain size of the previous austenite is inherited.

3. The reverted austenite is quite stable, does not transform to martensite on cooling, and therefore will not respond to aging. This is observed in a narrow band in the heat affected zone of welds.

### 3.4.2 MECHANICAL PROPERTIES

The high ductility and formability of the maraging steels in the martensitic (annealed) condition, combined with their high yield strength capability as-aged give these materials great advantage over both Group I and II steels. Thus, the heat treatment is simple, involves less warpage and dimensional problems and decarburizing possibilities. Moreover the maraging steels are readily weldable, requiring no pre-heating to promote formation of bainite, as in Group I steels. All of these characteristics confer on the material a high degree of amenability to the "roll and weld" process, which is mandatory for very large motor cases.

The most outstanding characteristic of the maraging steels (Group III) is their exceptionally high fracture toughness at high yield strengths. For example, Figure 28 shows the effect of test temperature on the tensile and Charpy V-notch impact properties of a typical 18 Nickel maraging steel. It will be noted that at a level of 245 ksi the corresponding impact strength is about 20 ft-lbs, a value not significantly different from that ordinarily obtained in a low alloy steel such as D6A-C, heat treated to the same yield strength. The fracture toughness-yield strength relations for the 18 Nickel maraging steels, based on the information available in the literature, are shown in Figure 29. It is seen that the average value at a yield strength of 245 ksi is about 120 ksi  $\sqrt{\text{in.}}$  compared to the value 60 ksi  $\sqrt{\text{in.}}$  for the D6A-C steel (Figure 12). The high degree of scatter will be discussed in the next section under Behavior. It is now interesting to compare the average curve of  $K_{IC}$  vs yield strength for the maraging steels (Group III) with those for Groups I and II (Figure 30). It is noted that for any level of yield strength below 200 ksi there are several materials which offer a range of fracture toughness, with the maraging steels enjoying a large margin in fracture toughness over all other steels at all levels of yield strength. In general, there appears to be a trend toward higher toughness with increasing nickel content, lower carbon, and possibly lower chromium. The high degree of reliability and amenability to the "roll and weld" process of the maraging steels establishes this class as a major candidate for large rocket motor case applications. As will be noted from Figure 30 at yield strengths greatly above 200 ksi say at 250 ksi, it is unique.

### 3.4.3 BEHAVIOR

Attention is called to the high degree of scatter in the data of Figure 29, the basis of which has been partly discussed in connection with the variations noted in the fracture toughness of the steels of Group I. Since the maraging steels are precipitation hardening alloys it is to be expected that response to aging would be greatly influenced by the thermomechanical variables of processing history. Compositional variables from heat to heat (particularly with respect to molybdenum, cobalt, and titanium) further complicate the picture. Thus, considerable variations in behavior between heats melted and processed

to a nominal yield strength are to be expected. There is, however, an important additional factor, especially characteristic of maraging steels which can contribute heavily not only to scatter of properties but also has an appreciable effect on the fabrication characteristics. This is banding, and the consequent anisotropy of fracture toughness.

In the conversion of the cast ingot of maraging steel to plate by hot working (rolling) the pattern of interdendritic micro-segregation of certain alloying elements is not completely diffused, but becomes flattened and elongated in the rolling plane and direction. Therefore the chemical heterogeneity manifests itself in the final microstructure as bands. Typical of the latter are those of Figure 31 and in Figure 32. The former are unidentified, but in the latter the white bands have been identified as residual austenite, stabilized by a segregation of alloying elements. This is confirmed by electron microprobe analysis carried out by Pelissier and his associates who reported persistent segregation of nickel, molybdenum and titanium in the austenitic bands (Figure 32). The role of such bands of austenite in fracture toughness tests has been suggested by Pelissier who pointed out that "internal shear lips" and "splits", observed in the fractures of longitudinal tensile test specimens cut from rolled plate, were oriented parallel to the rolling plane and direction (see Figure 33). On the basis of these observations and the reported discrepancies in fracture toughness resulting from different pre-cracked specimen geometries, he carried out fracture toughness tests on pre-cracked tensile specimens cut from 1 1/8-in. plate, of maraging (250 ksi) steel, oriented as indicated in Figure 34. The plane strain fracture data is given in Figure 34 from which it will be noted that the A and B values are essentially the same but that of the "C" value is about 12 percent higher. These data indicate quite clearly that a decrease in fracture toughness occurs when the crack propagates parallel to the bands, and that anisotropy must be taken into account when fracture toughness is evaluated.

The application of concentrated heat sources such as the plasma cutting torch, or high intensity welding arc to 18 Nickel maraging steel may cause this material to de-laminate or crack severely, in the heat affected zones (Figure 35). The severity of the problem will depend upon the thickness and degree of banding. It appears that the condition is essentially one of thermal shock, arising from the stresses between alternate layers of material with different physical and mechanical problems. This manifestation of anisotropy becomes a serious problem when considering the more rapid rate deposition processes such as submerged arc welding.

Studies on the stress-corrosion characteristics of maraging steels have been reported by a number of investigations (References 29, 30 and 31). The results of the investigation by Rubin are summarized in Figure 36. This data indicates that as the strength increases, the time for failure decreases, although there are great variations in resistance to delayed failure between the nine heats tested. The data also show that the 18 Nickel maraging steel is more resistant than the low alloy steels when compared at the same strength level.

#### 3.4.4 WELDABILITY

The most satisfactory welds (soundness, and fracture toughness) in 18 percent nickel maraging steels, to date, have been made by the TIG welding process. Although the fracture toughness is generally appreciably lower in the weld metal than in the parent metal, the difference becomes smaller at the lower yield strength levels. For example, Masters (Reference 25) reports values of  $K_{IC} = 164 \text{ ksi } \sqrt{\text{in.}}$  and  $131 \text{ ksi } \sqrt{\text{in.}}$  for parent and weld metal respectively in 3/4-in. plate of 200 ksi yield strength. Romine (Reference 26)

conducted weld studies on 1/2-in. thick plate of 250 ksi yield strength and obtained a range of 73 to 93 ksi  $\sqrt{\text{in.}}$  for parent metal and 46 to 63 ksi  $\sqrt{\text{in.}}$  in the weld metal. His joint efficiencies were 96 percent on a yield strength basis and 90 to 94 percent on a tensile strength basis.

It has been reported (Reference 33) that filler metals of base compositions with lower molybdenum content (4.5% in filler compared to 5.0% in plate) will improve notch toughness, and with higher titanium and aluminum contents will provide thorough deoxidation of the weld and prevent hot cracking. Vacuum melted filler wires are preferred because their lower hydrogen content (less than 5 ppm) eliminates transverse weld cracking, particularly in welding 1/2-inch or over thick sections (References 33 and 34). With these filler compositions weld properties furnished in Table 5 can be obtained.

Welding studies (Reference 35) on the maraging steels have shown that a narrow light-etching region of stable austenite (impaired heat-affected zone in Figure 37) is in the base metal or weld metal (as in multipass welds) sections heated to 1100° and 1200°F during welding. This stable austenite, reverted from pre-existing martensite, does not respond to subsequent aging treatments and is therefore tougher but not as strong as the aged material. Tensile failures have been reported (Reference 30) to occur in this austenitic zone.

To minimize the reverted austenite problem, the following weld precautions have been recommended.

1. To avoid preheating; use 250°F maximum interpass temperature.
2. Use minimum possible weld-energy input. This imposes a problem when high energy metal deposition processes such as submerged arc welding are necessary.
3. Avoid other conditions causing low cooling rates or prolonged times in the 1100°F to 1200°F temperature range.

Because of the slow speed and cost of the TIG process, MIG welding is being studied for application to welding of the nickel maraging steels. However, conventional direct-current MIG welding is associated with magnetic arc blow, arc wandering and weld unsoundness and, therefore modifications of MIG welding are under investigation. It has been observed that MIG weld metal with 1.2 percent titanium is far less sensitive to changes in aging treatment (after welding) than weld metal with 0.5 percent titanium. This appears significant, especially in fabrication of components involving prolonged aging treatments, such as intersecting welds or repair welds.

Preliminary evaluations (Reference 36) of the electron beam method for welding 1/2-inch 18 Ni (250) and 1-inch 18 Ni (300) indicated joint strengths equal to the unwelded parent material on aging after welding. There was also a loss in elongation and reduction of area in the weld that is not recoverable by heat treatment. While no fracture toughness results have been reported for electron beam welds, a preliminary basis for comparison of this type of joining with MIG welding is shown in Figure 38, in which tensile fracture stress is plotted against specimen crack depth for a number of weld tests and techniques. It is indicated that resistance to catastrophic crack propagation is essentially independent of the two weld metal composition and deposition techniques. Figure 38 shows that crack size for crack propagation in the weld is about 0.028 to 0.038-inch compared to a base metal value of about .080 in. This data must be considered preliminary.

## 4. DESIGN CONSIDERATIONS

### 4.1 MATERIAL RELIABILITY COMPARISON

In the section on Reliability and Reliability Parameters an equation was derived:

$$\left(\frac{a}{Q}\right)^{1/2} = \frac{K_{IC}}{1.1 \sqrt{\pi} \sigma} \quad \text{where } \sigma \text{ is the design}$$

or operating stress,  $K_{IC}$  the plane strain fracture toughness and  $\frac{a}{Q}$  the relative flaw size. The value of  $Q$ , the flaw shape parameter depends on the dimensions of the defect and the ratio of  $\sigma$  to the yield strength.

By using the yield-strength-fracture toughness relations of Figure 30, the operating stress can now be plotted as a function of relative flaw size for any of the steels of Groups I, II and III, at a particular strength level. Figure 39 compares all of these steels, at a yield strength level of 200 ksi. This is therefore a quantitative reliability comparison, considerably more useful to the designer than Figure 30. The parameter  $K_{IC}$  is indicated for each steel of Figure 30, but the designer is free to select others (or perhaps the entire scatter-band) of Figures 12, 13, 14, 15, 22 and 29 for each steel of interest to him.

### 4.2 MAXIMUM STRENGTH-TO-WEIGHT VS MAXIMUM RELIABILITY

In Figure 40 is plotted the wall thickness as a function of yield strength for pressure vessels (cases) of 60, 120 and 260 inches in diameter, operating at an internal pressure of 660 psi, and a design proof stress of 0.82 times the yield strength. If a semi-elliptical crack having a depth to length  $a/2c =$  approximately  $1/7$  is assumed, then, for an operating stress = 0.82 times the yield strength, the flaw shape parameter = 1. In Figure 38 are superimposed the relations between yield strength and critical flaw size for each of three steels (D6A-C, HP-9-4-25 and 18 Nickel maraging steel). From these curves a table showing the maximum tolerable crack depth is derived. Table 6 compares the crack depth and case thickness at 200 and 250 ksi yield strength levels. It is seen that at 200 ksi, in all steels, the critical crack depth is within ordinary limits of non-destructive inspection. On the other hand at 250 ksi, the critical flaw size in the maraging steel has gone down to about  $1/5$  the value at 200 ksi whereas for the D6A-C steel the flaw size is outside ordinary inspection limits.

It is interesting to note the trade-off for the maraging steel. In achieving a 20 percent reduction in weight, the reliability has been reduced. These considerations will be influenced substantially by the degree of scatter (see Figures 12-15, 22 and 29). Furthermore the properties of the welded joints must also be taken into account. The designer must decide whether the gain in payload is worth the reduced reliability.

The comparisons and discussions up to now have been based on the mechanical properties of wrought metal. It has already been pointed out that for any motor case which is too large for shear spinning, extensive longitudinal welding ("roll and weld") will be necessary. Therefore, in assessing potential reliability of a fabricated case, the properties of the weld-metal (particularly its fracture toughness) must be considered, especially since the presence of a defect is much more probable in the weld metal than in the parent metal. Unfortunately there is a paucity of yield strength-fracture toughness

data on weldments of the steels considered in this paper. Table 7 presents a compilation of the available data on welds and parent metal of a number of these steels. Attention is called to the critical (or tolerable) crack length, calculated from the given values of yield strength,  $K_{IC}$ , and the assumed ratio of  $\frac{a}{2c} = \frac{1}{7.15}$ , and applied stress = 0.82 times yield strength.

The data indicate that at the lower yield strengths the critical crack length of the weld metal approaches that of the parent metal, but at higher values of yield strength it can be appreciably lower. Therefore, as before, the designer must use great caution in going to higher yield strength materials in the design of large welded motor cases. He is on much safer ground when he restricts his use of the very high yield strength materials to motor cases where shear spinning is involved and only girth welds are involved, and savings in weight are more effective.

## REFERENCES

1. Esgar, J. B., Dow, N. F., and Micks, "Recommendations and Evaluations of Material-Research Areas of Importance to Missile and Space Vehicle Structures" NASA Technical Note NASA TN-D-2125 October 1963.
2. DMIC Report 180, "Design Considerations in Selecting Materials for Large Solid-Propellant Rocket-Motor Cases" December 10, 1962.
3. Abraham, L. H., "Structural Design of Missiles and Spacecraft", McGraw-Hill Book Co. Inc., New York, 1962, pages 182 - 184.
4. Kinnamen, E. B., Jacobsen, R. E. and Tiffany, C. F., "An Approach to the Practical Design of Light Weight, High Strength Pressure Vessels". IAS Paper No. 59 - 109, Los Angeles, California, June 16, 1959.
5. Dyar, J. R. and Bratkovich, N. F., "Reliable Weld Joint Design for High Strength Rocket Motor Cases". Welding Research Vol. XXVIII, No. 3 March 1963.
6. Williams, H. L., "On the Stress Distribution at the Base of a Stationary Crack", Journal of Applied Mechanics, March 1957.
7. Irwin, G. R., "Analysis of Stresses and Strains Near the End of a Crack Traversing a Plate". Journal of Mechanics, September 1957.
8. ASTM Materials Research and Standards" Vol. 1 No. II (Pages 885-887) November 1961, Vol. 2 No. 3 (Pages 196-203) March 1962 and Vol.4 No. 1, January 1964.
9. DMIC Report 200, "Vacuum Degassing in the Production of Premium-Quality Steels" March 1964.
10. Wei, R. P., "Fracture Toughness Testing in Alloy Development". Seventh Annual Meeting ASTM, Chicago, Illinois, June 21-26, 1964.
11. Hanna, G. L. and Steigerwald, E. A. "Influence of Environment on Crack Propagation and Delayed Failures in High-Strength Steels" Technical Documentary Report RTD-TDR-63-4225 January 1964.
12. Alexander, R. V. and Fourmer, C. A. "Cost and Performance Considerations in the Selection of Structural Materials for Ultra-Large Size Booster Motors". Journal of Spacecraft and Motors, Vol. 1, No. 1 (Pages 62-67) January-February 1964.
13. Schwartzbart, H. and Rudy, J. H., "Welding Ultra-High Strength Steel Sheet". Welding Research Council of Engineering Foundation Bulletin 79. July 1962.
14. Aborn, R. H. "Low Carbon Martensites", Transactions of the American Society for Metals, Vol. XLVIII, 1956.

## REFERENCES (CONT'D)

15. Reis, G. D. and Poole, S. W., "Welding of HP-9-4-X Alloy" Fourth Maraging Steel Project Review, June 9-11, 1964, Dayton, Ohio. (ML-TDR 64-225).
16. Munger, H. P., "HP 150-An Alloy with High Strength and Maximum Toughness" Fourth Maraging Steel Project Review, June 9-11, 1964, Dayton, Ohio. (ML-TDR-64-225).
17. Crimmins, P. P., "Evaluation of High Nickel Steel for Application in Large Booster Case Materials." Third Maraging Steel Project Review, Report No. RTD-TDR-63-4048 (Air Force Materials Laboratory, Wright-Patterson Air Force Base, Ohio) pages 95-183, November 1963.
18. DMIC Report 198, "The Mechanical Properties of the 18 Per Cent Nickel Maraging Steels" (page 12) February 24, 1964.
19. Pellissier, G. E., "Some Microstructural Aspects of Maraging (250) Steel in Relation to Strength and Toughness" Third Maraging Steel Project Review, Report No. RTD-TDR-63-4048 (Pages 439-455) November 1963.
20. Kula, E. B. and Hickey, C. F., Jr., "Evaluation of Maraging Steel at U. S. Army Watertown Arsenal, Watertown, Massachusetts", Third Maraging Steel Project Review, Report No. RTD-TDR-63-4048, Air Force Materials Laboratory, Wright-Patterson Air Force Base, Ohio, pages 439-455, November 1963.
21. Tiffany, C. F. and Lorenz, P. M. "An Investigation of Low-Cycle Fatigue Failures Using Applied Fracture Mechanics". Air Force Materials Laboratory, Wright-Patterson Air Force Base, Ohio Technical Documentary Report ML-TDR-64-53.
22. Pascover, J. S., Matas, S. J., and Barclay, W. F. "Tough High-Strength Steels for Aerospace Applications". Sixth Symposium of the Society for Aerospace Materials and Processing Engineers. November 18, 1963.
23. Hanna, G. L. and Steigerwald, E. A., "Fracture Characteristics of Structural Metals", Report ER-5426 (Contract No. N600(19)58831) June 30, 1963.
24. Amateau, M. F., Hanna, G. L., and Steigerwald, E. A., "Fractural Characteristics of Structural Metals" Report ER-5927 (Contract NOw-64-0186c) April 30, 1964.
25. Masters, J. N. "Booster Case Materials Evaluation". Fourth Maraging Steel Project Review, June 9-11, 1964, Dayton, Ohio (ML-TDR-64-225).
26. Romine, H. E. "Plane Strain Fracture Toughness Measurements of Solid Booster Case Materials" Third Maraging Steel Project Review RTD-TDR-63-4048, November 1963.
27. Melville, A. "Metallurgical Evaluation of 18% Nickel Maraging Steel (300 ksi Strength Level)" Third Maraging Steel Project Review RTD-TDR-63-4048, November 1963.

REFERENCES (CONT'D)

28. Owen, E. A., and Liu, Y. H., "Further X-Ray Study of the Equilibrium Diagram of the Iron-Nickel System", Journal of the Iron and Steel Institute, Vol. 163, 132-137 (1949).
29. Rubin, A., "Stress Corrosion Cracking of Maraging Steels". Fourth Maraging Steel Project Review, June 9-11, 1964, Dayton, Ohio (ML-TDR-64-225).
30. Saperstein, Z. P. and Whiteson, B. W., "The Properties of Welded 18 Ni-Co-5 Mo Plate". Third Maraging Steel Project Review, RTD-TDR-63-4048, November 1963.
31. Scharfstein, L. R., "Stress-Corrosion Cracking of 18% Nickel Maraging Steel". Journal of Iron and Steel Institute, 1964, Vol. 202, February, pp 158-9.
32. Pascover, J. S. and Matas, "Properties of HP-9-4-X Alloy Steels". Fourth Maraging Steel Project Review, June 9-11, 1964, Dayton, Ohio (ML-TDR-64-225).
33. Witherell, C. E., Corrigan, D. A., and Petersen, W. A., "Working with Maraging Steels - Welding". Metal Progress, July 1963.
34. Witherell, C. E., and Fragetta, W. A. "Weldability of 18% Ni Steel". Welding Research Supplement to The Welding Journal, November 1962.
35. Saperstein, Z. P., Whiteson, B. W. and Duffey, F. D., "Investigation of Properties and Fabricability of 3/4-Inch Thick Air-Melted 18 Ni-7 Co - 5 Mo Plate". Second Maraging Steel Conference, Dayton, Ohio, November 7-8, 1962.
36. Padien, W. D., Toy, A. and Robelotto, "Electron Beam Welding of One-Half Inch Thick Maraging Steel". Third Maraging Steel Project Review, RTD-TDR-63-4048, November 1963.
37. Trozzo, P. S. and Pellissier, G. E., "The Influence of Microstructure on Strength and Toughness of Low-Carbon, High Alloy Steels". AIME 1964 Fall Meeting Program, Page 20, Journal of Metals, September 1964.



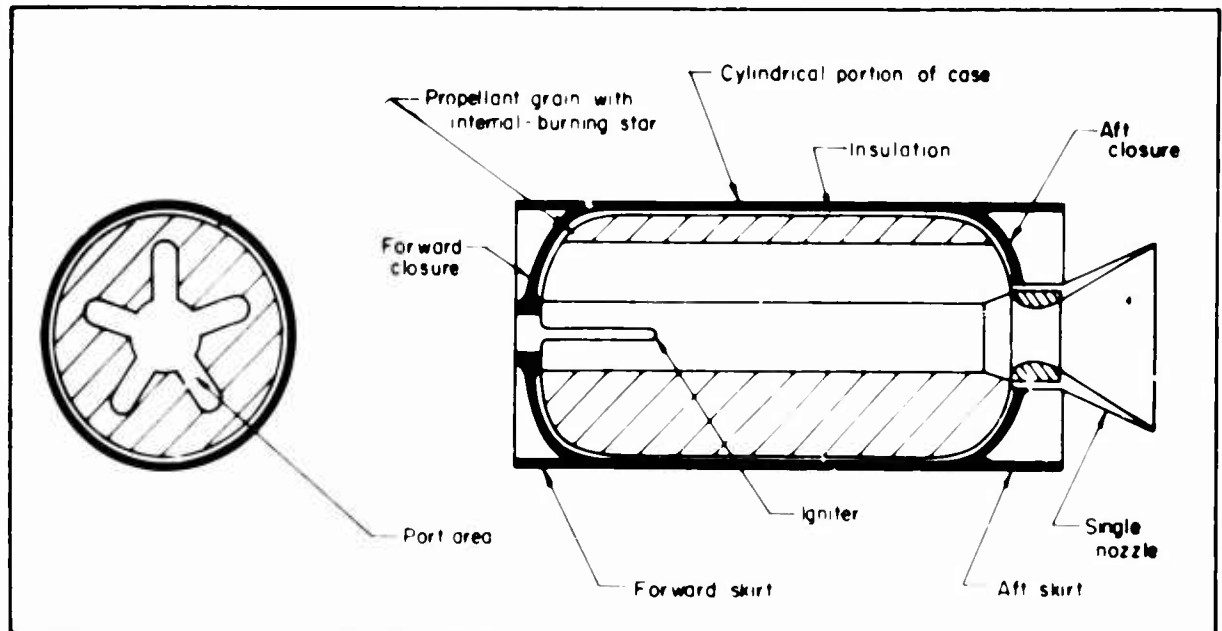


Figure 1. Typical Solid-Propellant Rocket Motor Including Case, Propellant and Nozzle

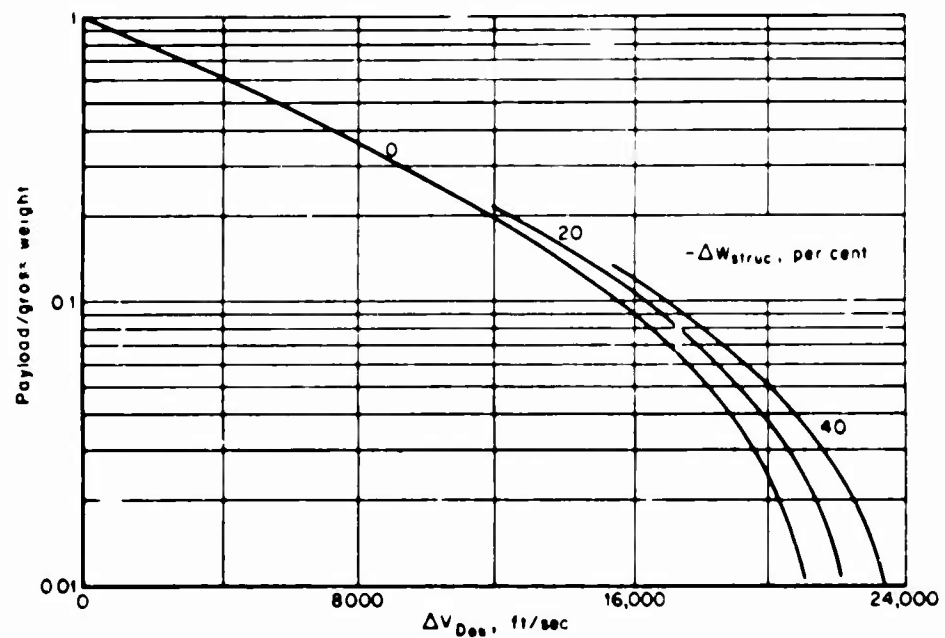


Figure 2. Performance Increases from Reduction of Structural Weight of First Stage of Typical Booster.

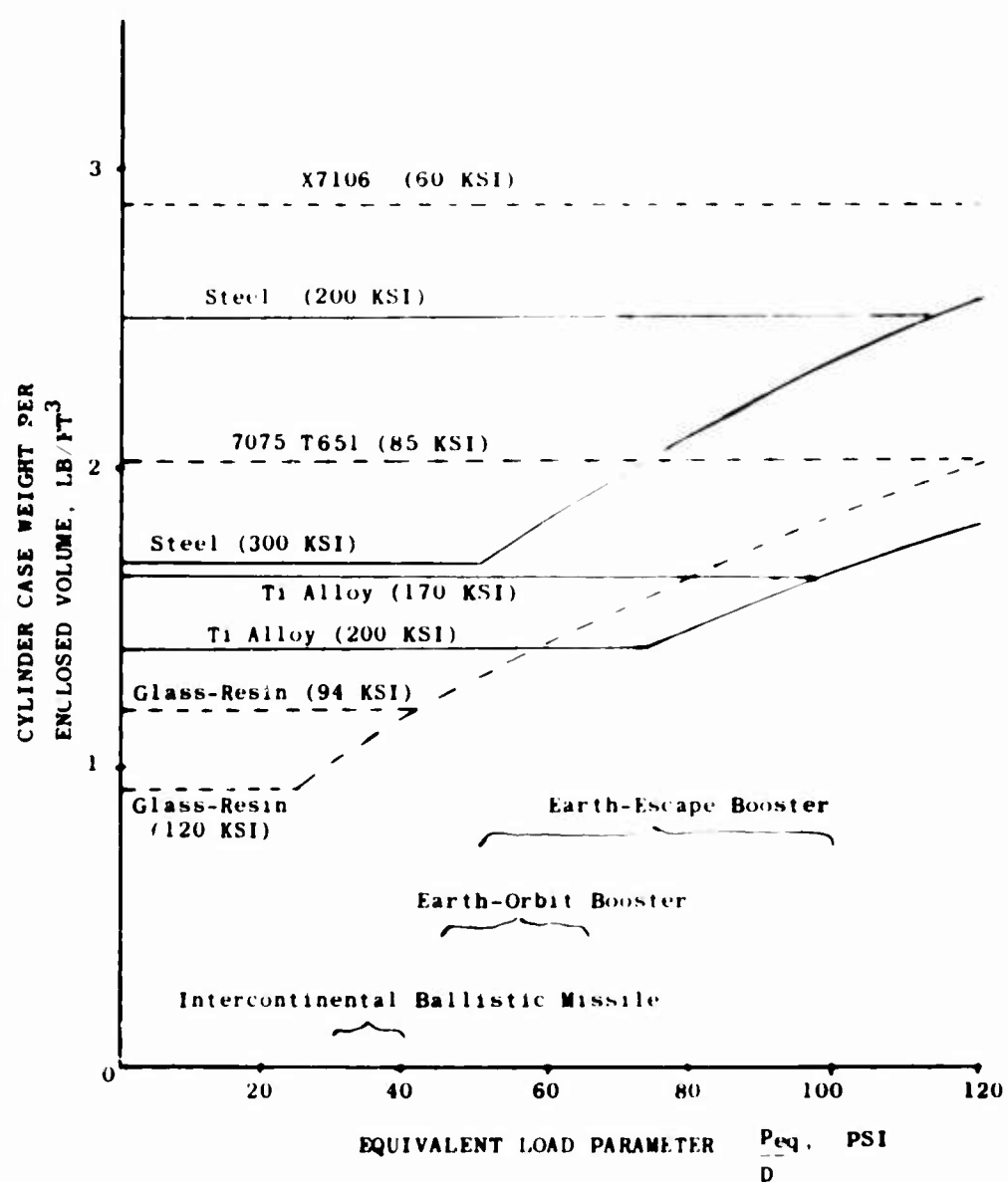


Figure 3. Weight of Cylindrical Portion of Rocket Motor Case Per Unit of Enclosed Volume Versus an Equivalent External Load Parameter (Internal Pressure = 400 psi)



Figure 4. 260" Diameter "Y" Ring Steel Forging

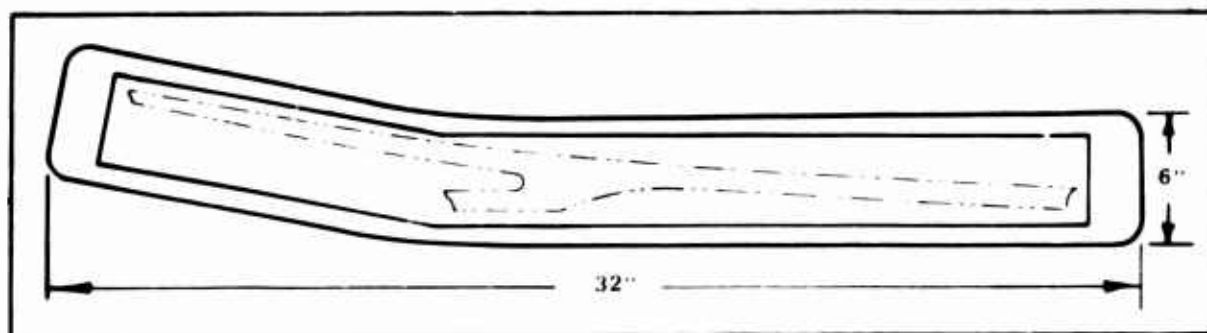


Figure 5. Cross-Section of 260" Diameter "Y" Ring

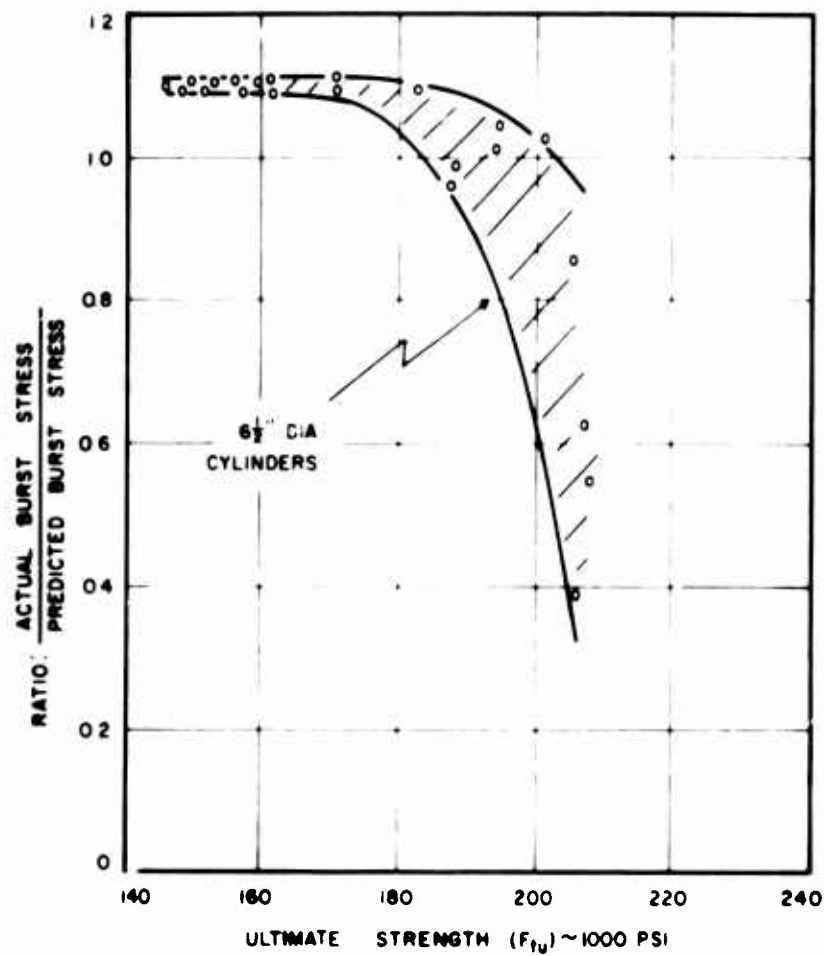


Figure 6. Burst Test Results for 17-7 PH Steel Tanks Tested at Room Temperature

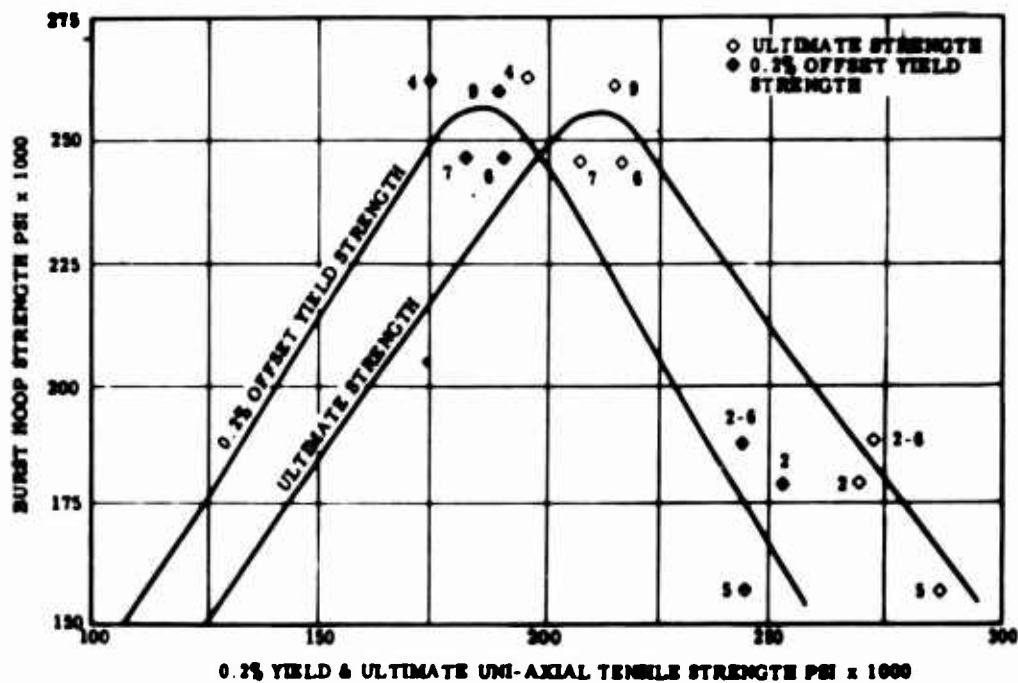


Figure 7. 0.2% Yield and Ultimate Unaxial Tensile Strength vs. Ultimate Burst Hoop Strength for 24 in. Diam. and 6.660 in. Diam. D6AC Subscale Test Vessels.

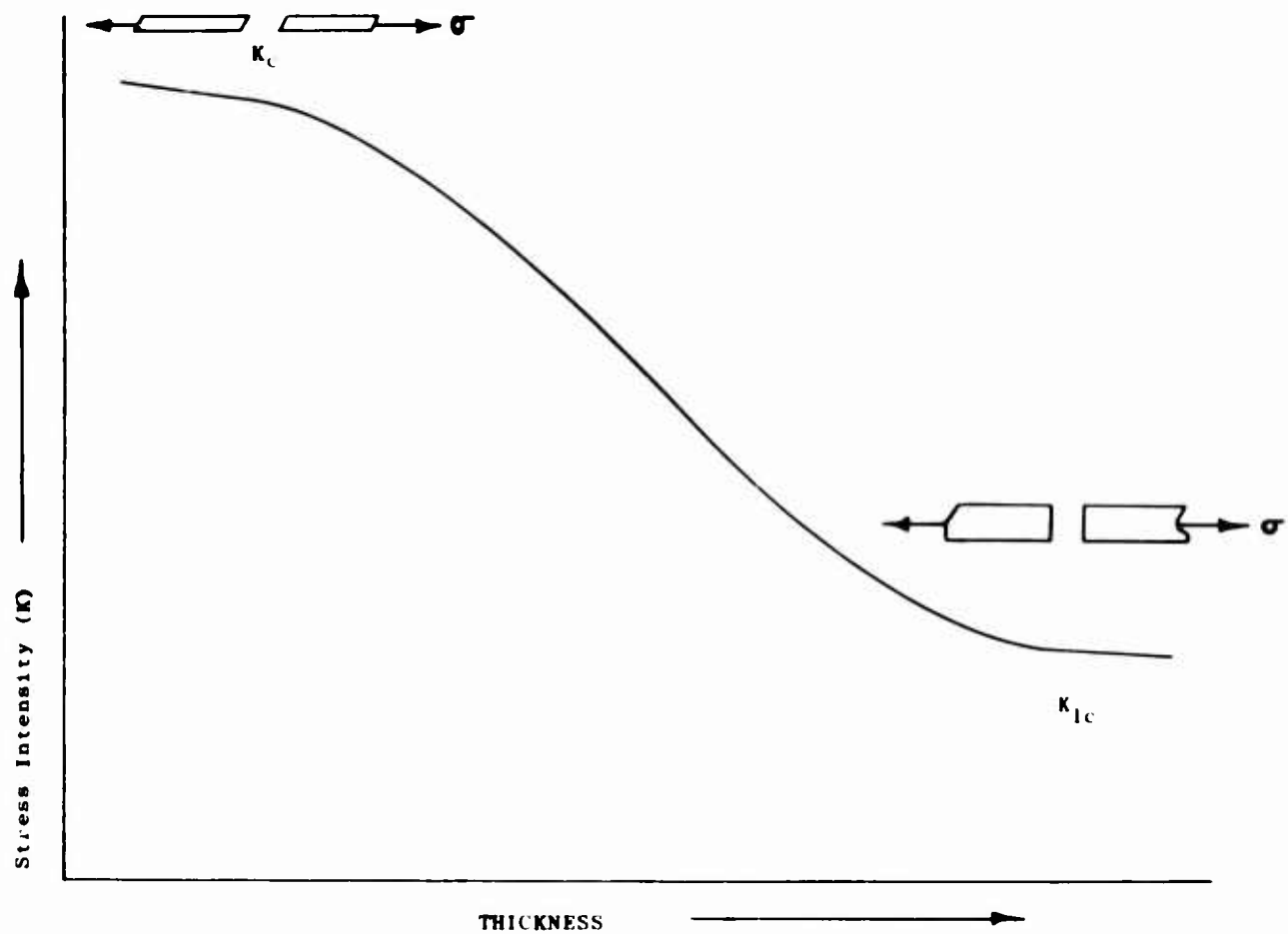


Figure 8. Fracture Mode Transition

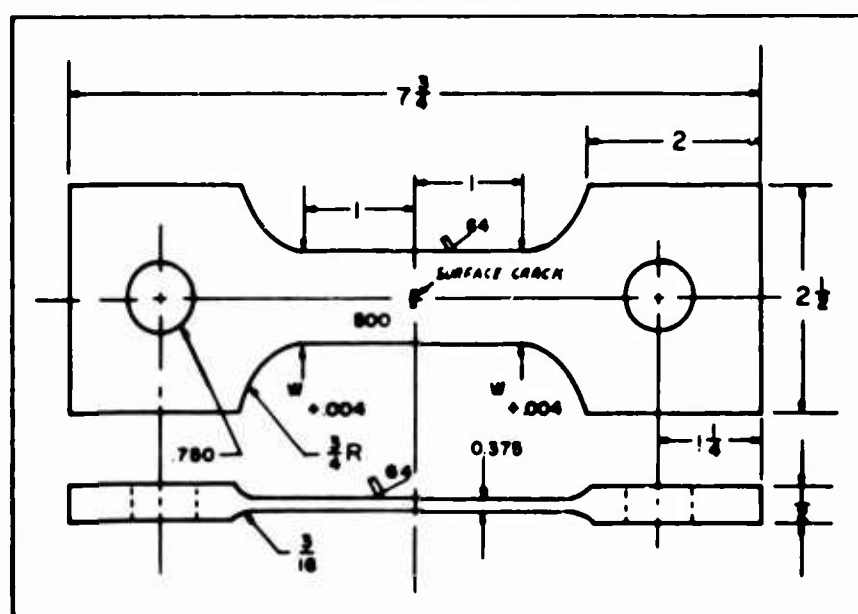


Figure 9. Surface-Cracked Specimen

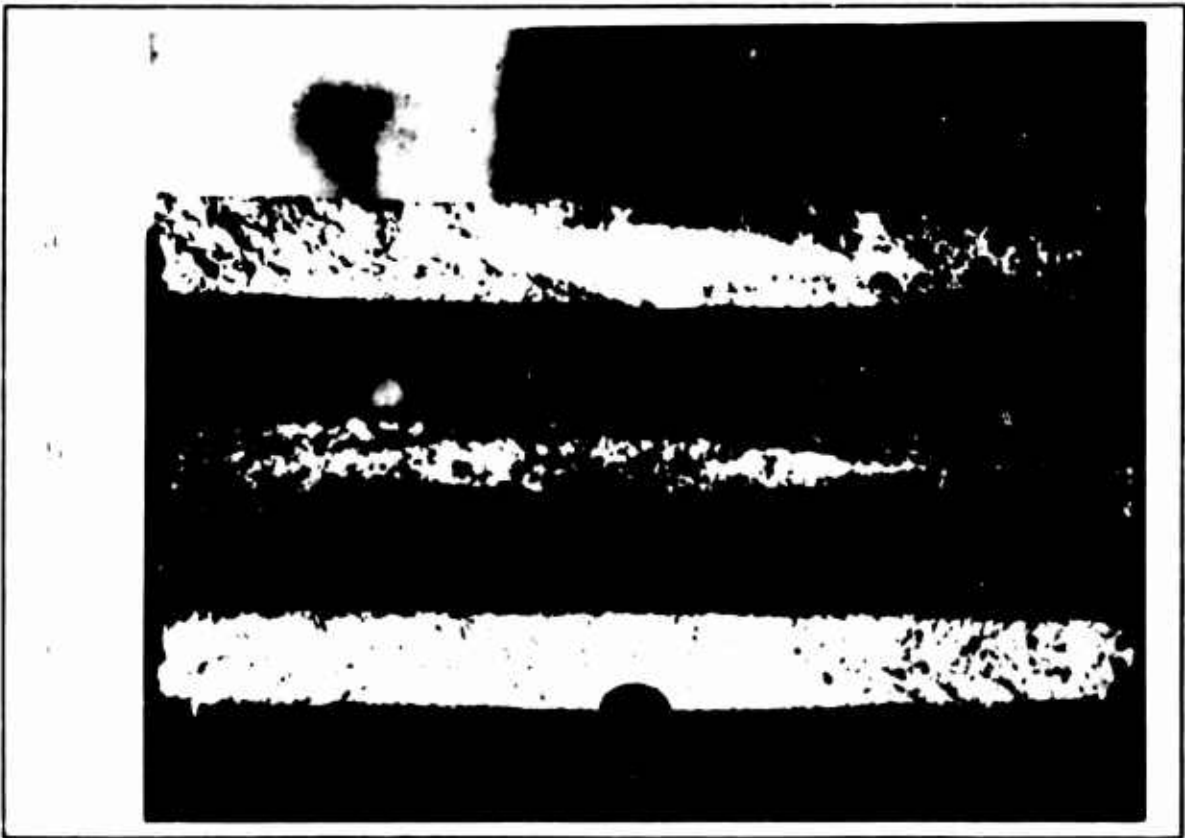


Figure 10. Surface-Cracked Fracture Toughness Specimens (a & b 4340 and C H11)

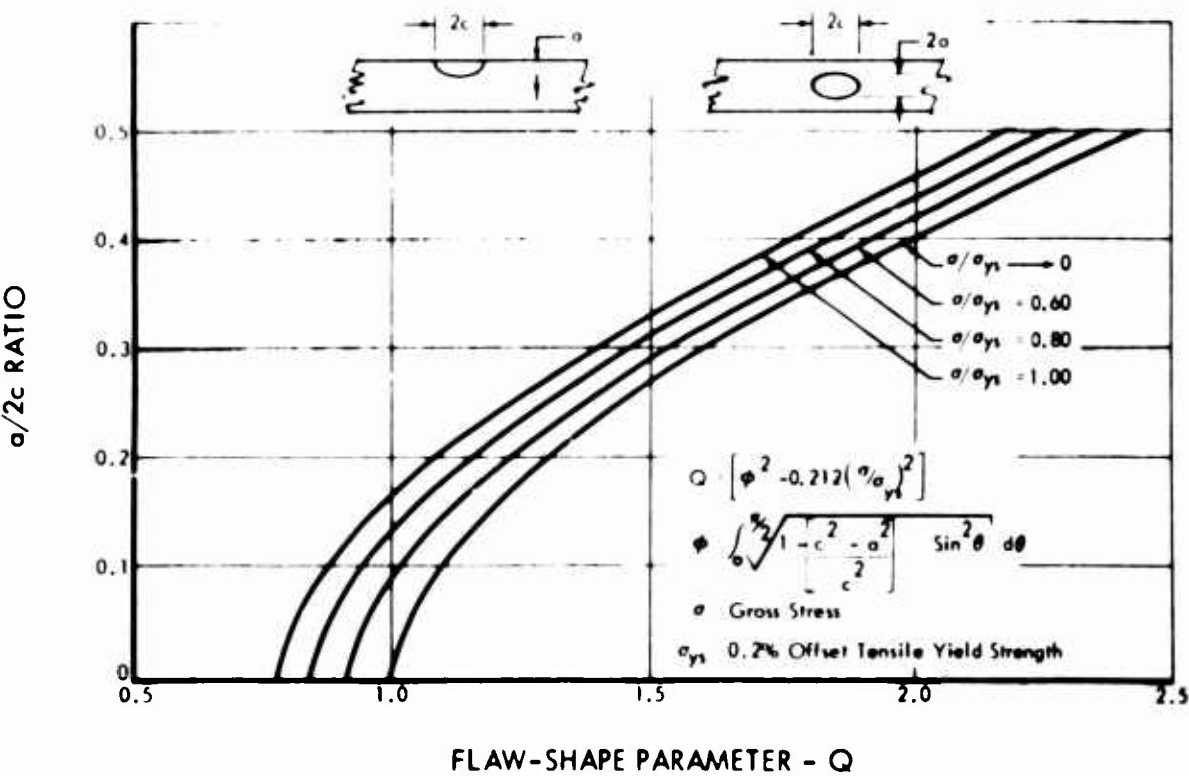


Figure 11. Flaw Shape Parameter Curves for Surface and Internal Cracks

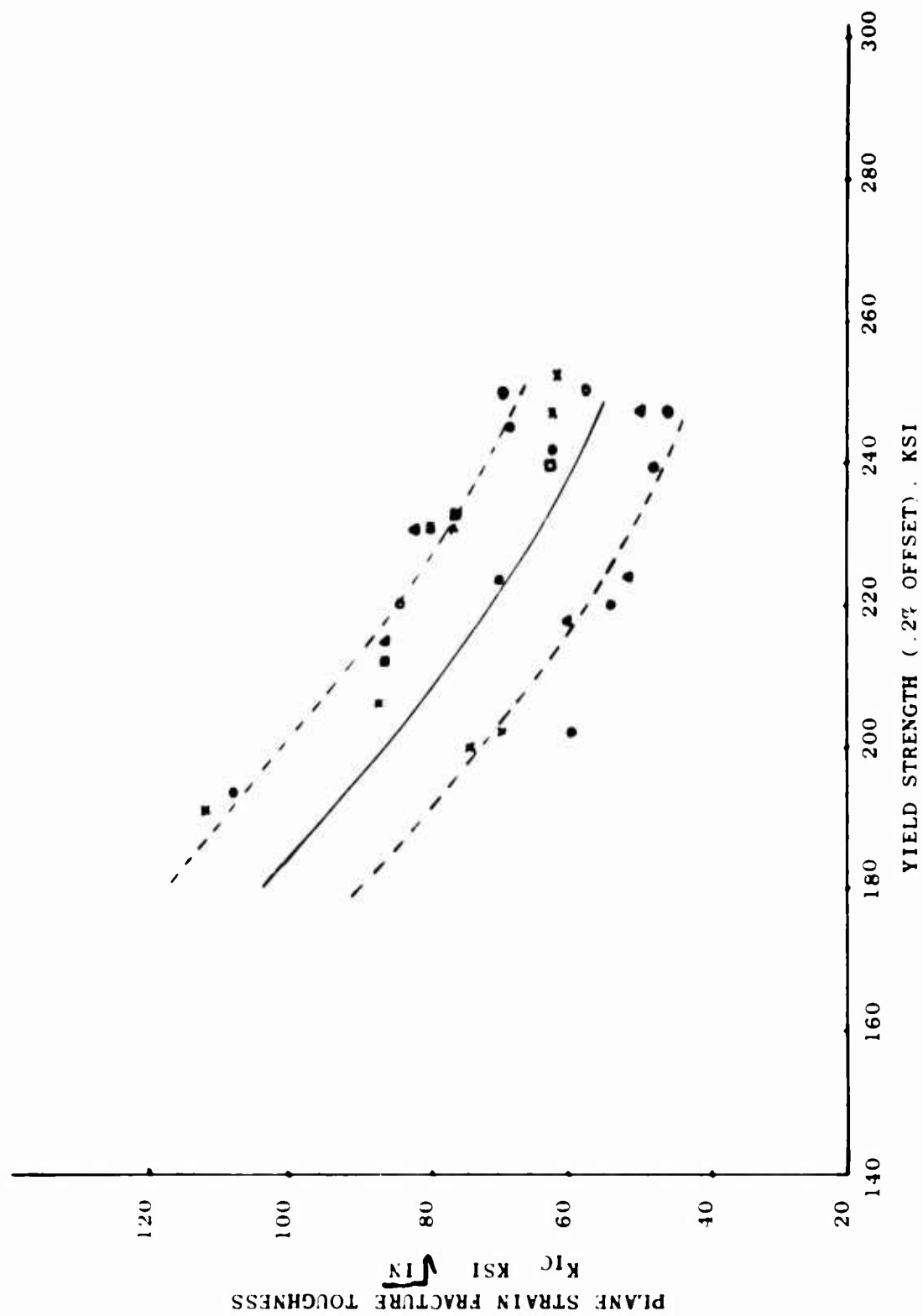


Figure 12. Range of Plane Strain Fracture Toughness Values,  $K_{IC}$ , for D6A-C Steel (References 21 and 22)

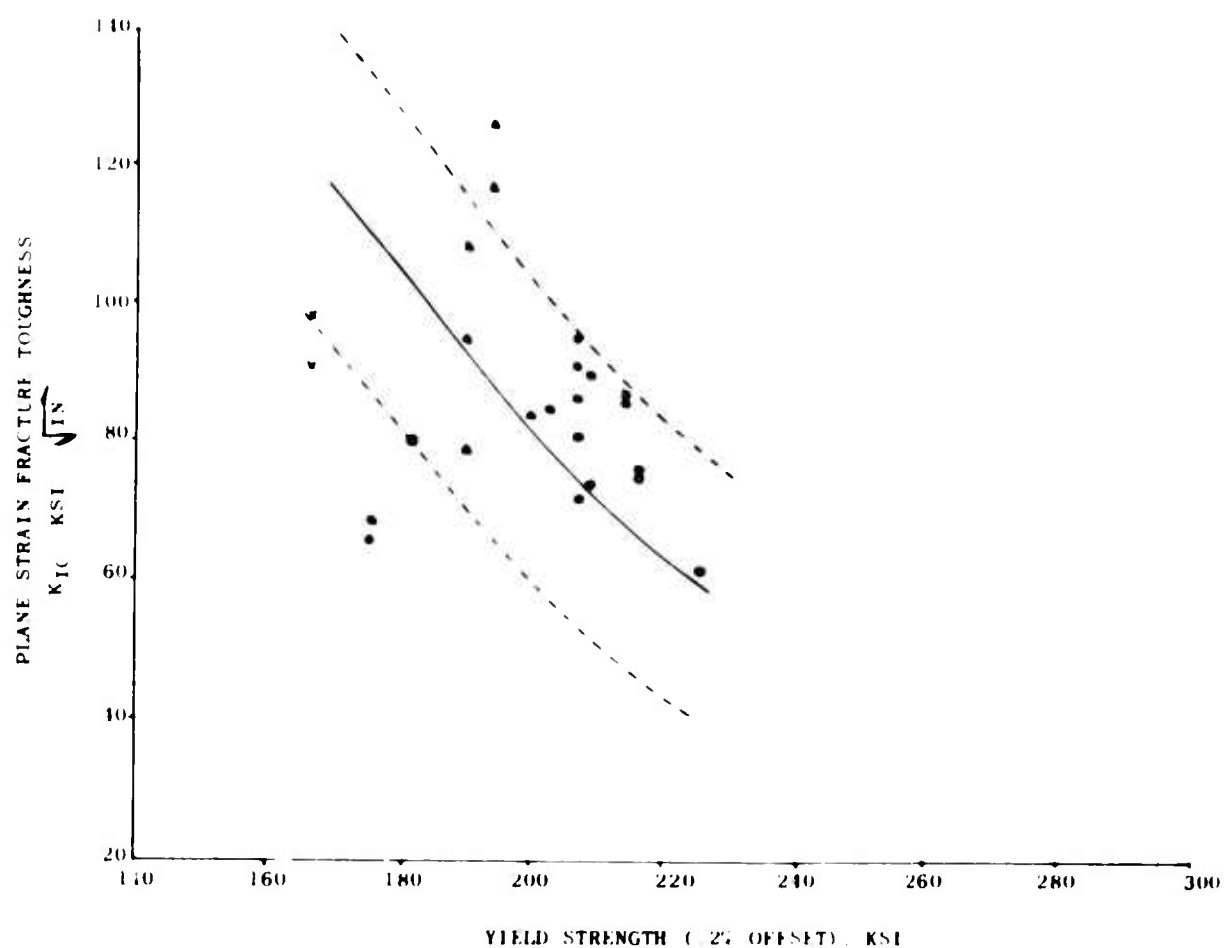


Figure 13. Range of Plane Strain Fracture Toughness Values,  $K_{IC}$ , for 4335V Steels (Reference 23)



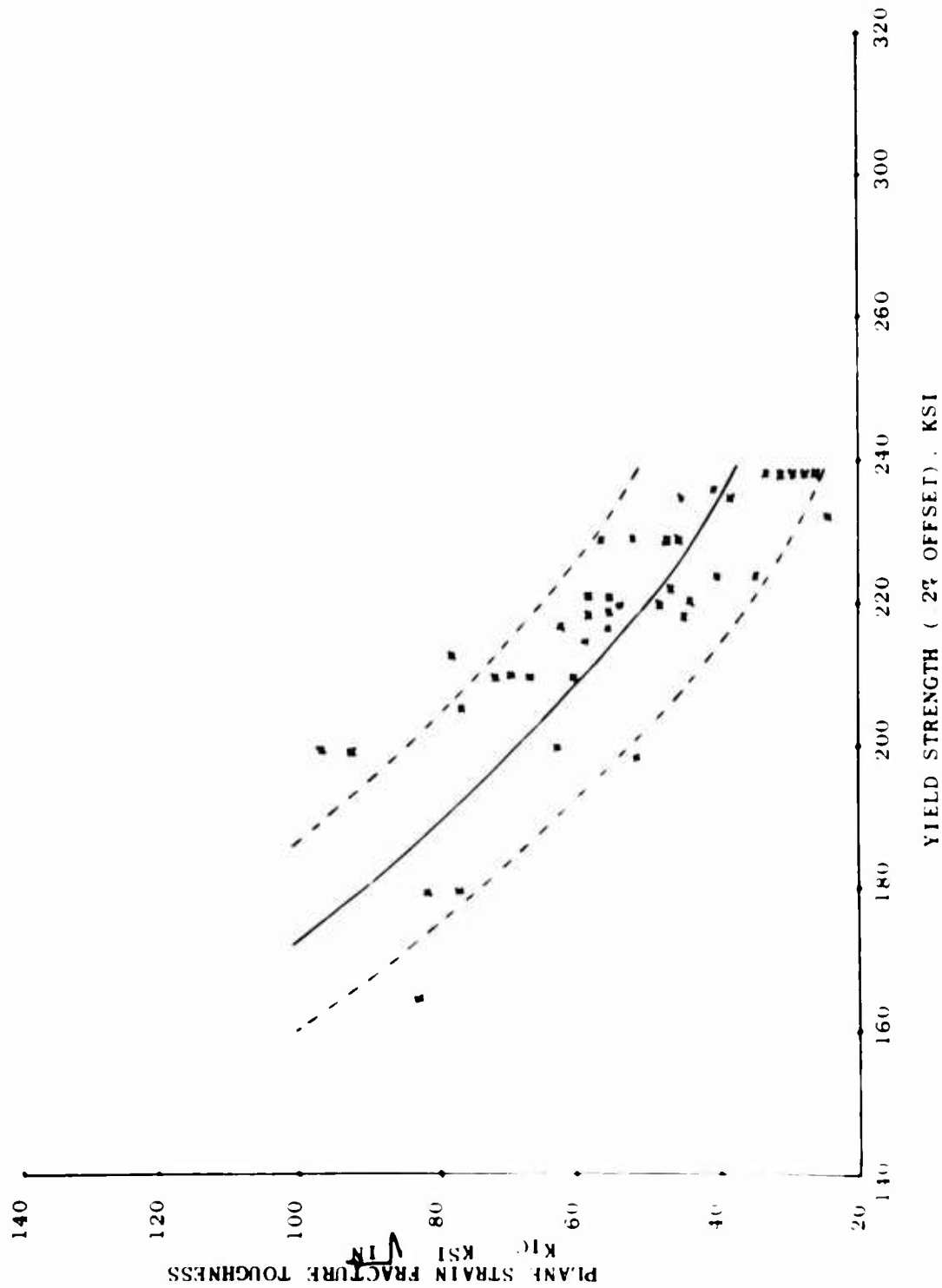


Figure 14. Range of Plane Strain Fracture Toughness Values,  $K_{IC}$ , for 4340 Steels.

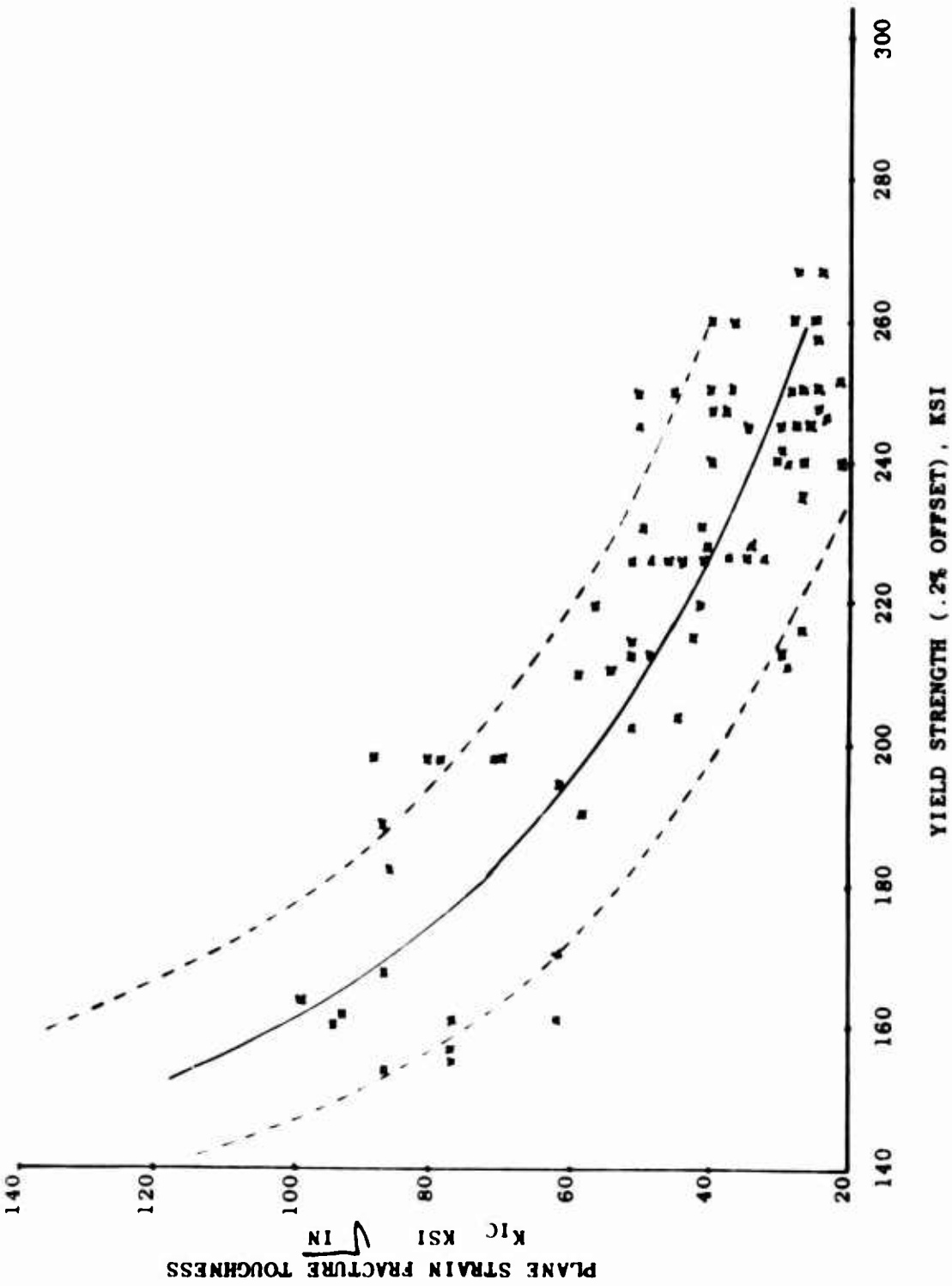


Figure 15. Range of Plane Strain Fracture Toughness Values,  $K_{IC}$ , for H11 Steels.

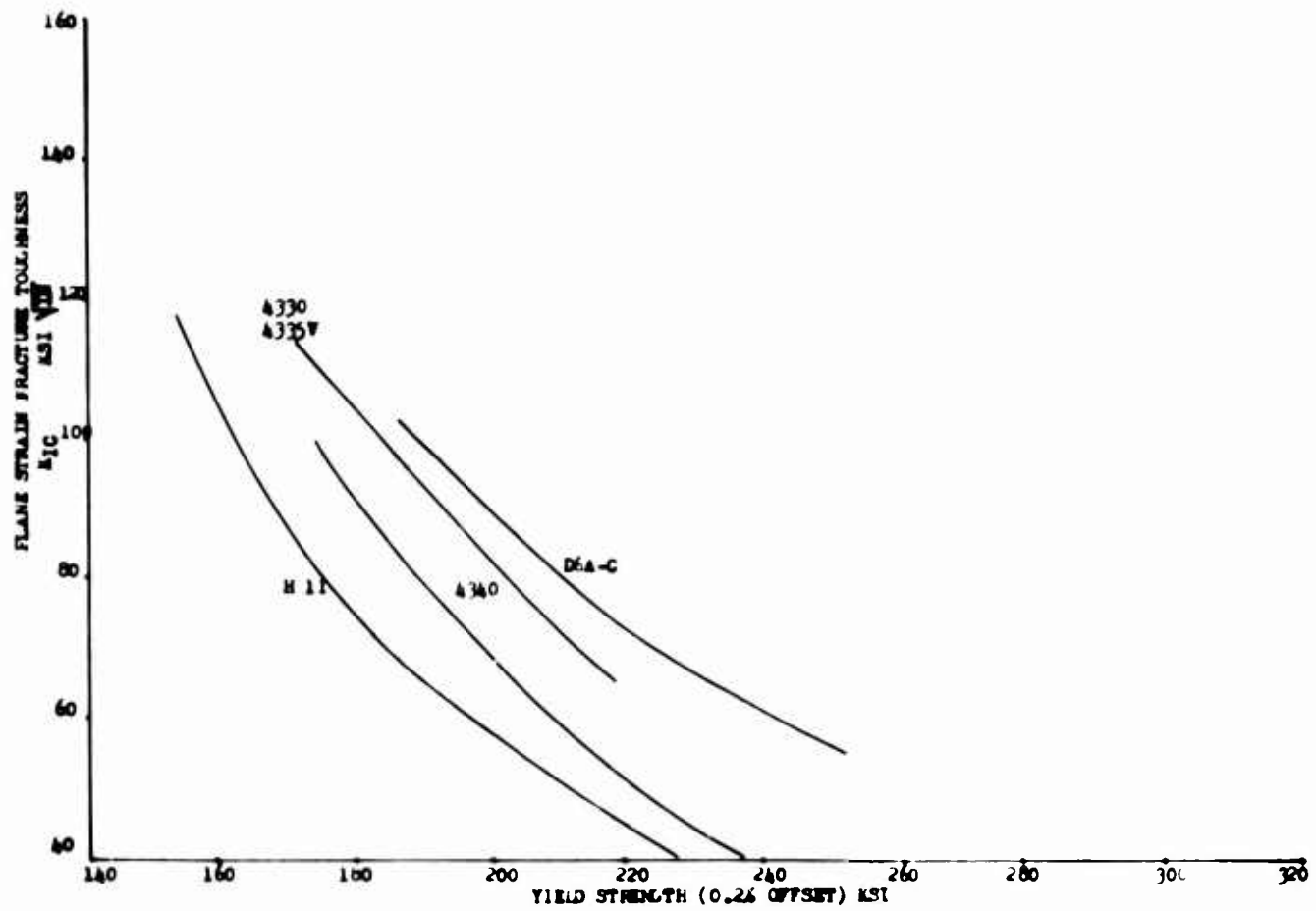


Figure 16. Average Plane Strain Fracture Toughness ( $K_{IC}$ ) Values for Group I Steels.

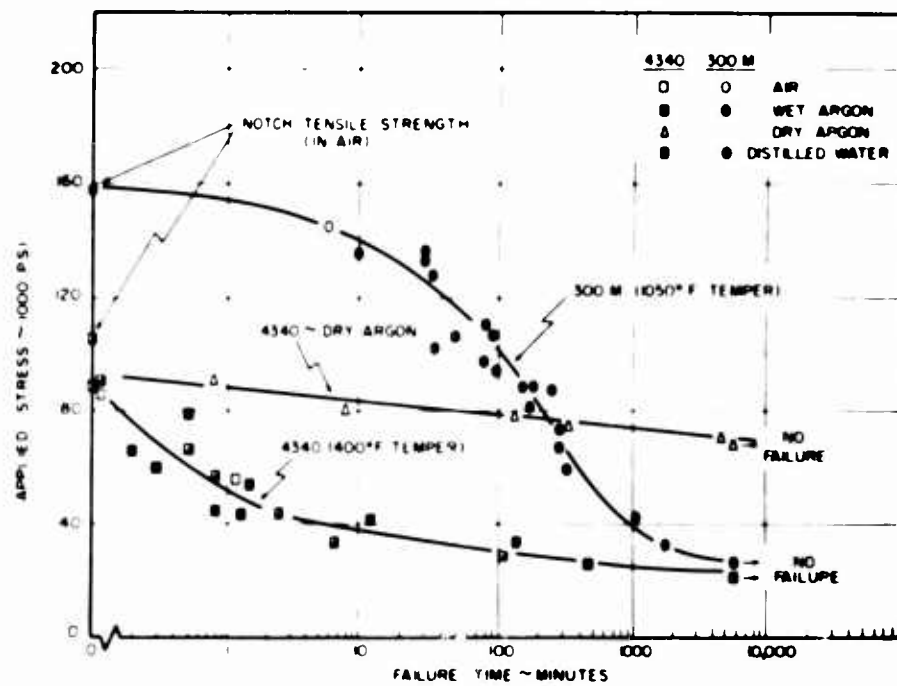


Figure 17. Comparison of Air, Argon and Distilled Water Environments on Delayed Failure Characteristics of 4340 and 300 M Steels at 68°F.

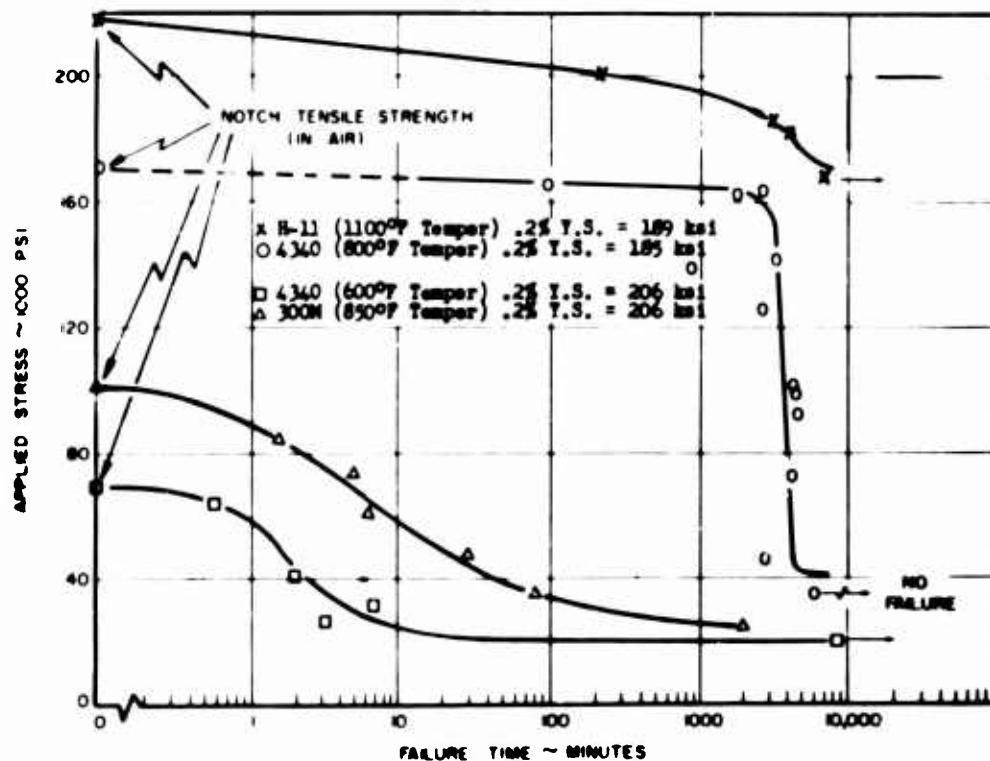


Figure 18. Delayed Failure Characteristics of 4340, 300 M and H-11 Steels, in Distilled Water at 68°F.

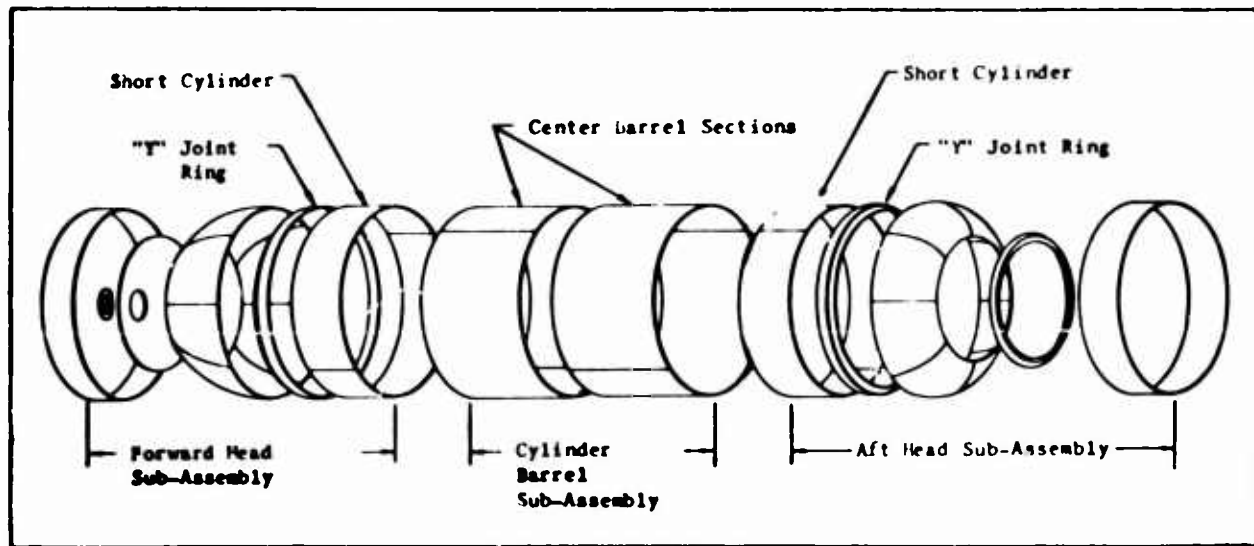


Figure 19. Segmented Chamber Construction

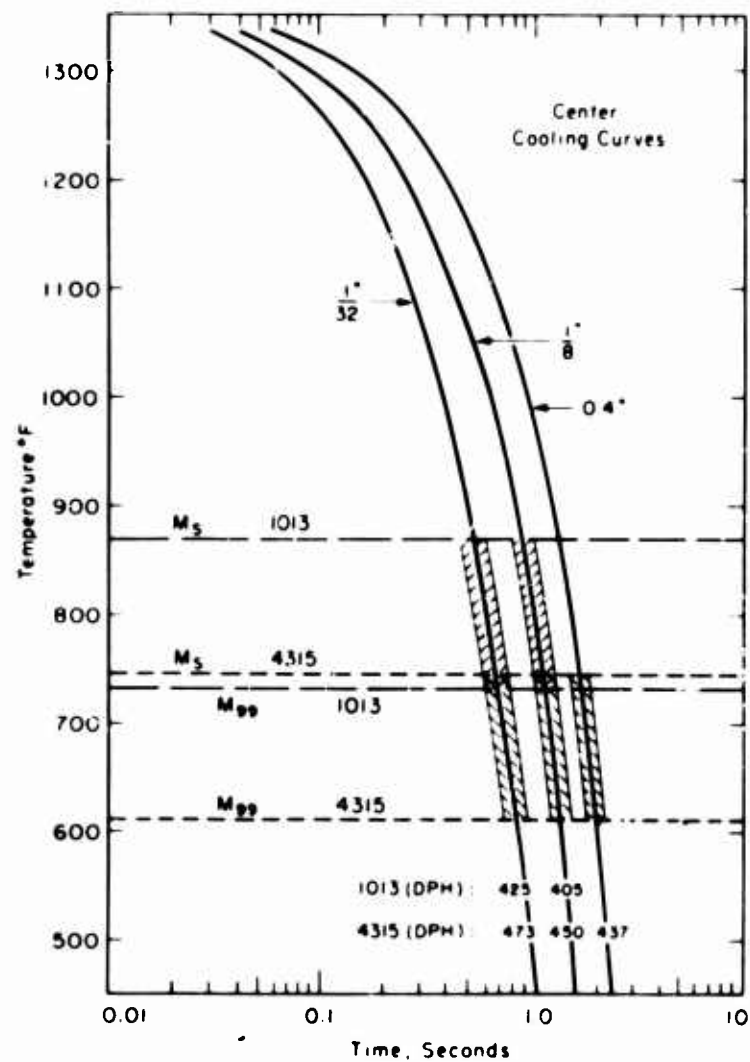


Figure 20. Temperature Range of Martensite Formation in 1013 and 4315 Steels and Idealized Cooling Curves for Each of Three Specimen Thicknesses Quenched in Ice-Brine.

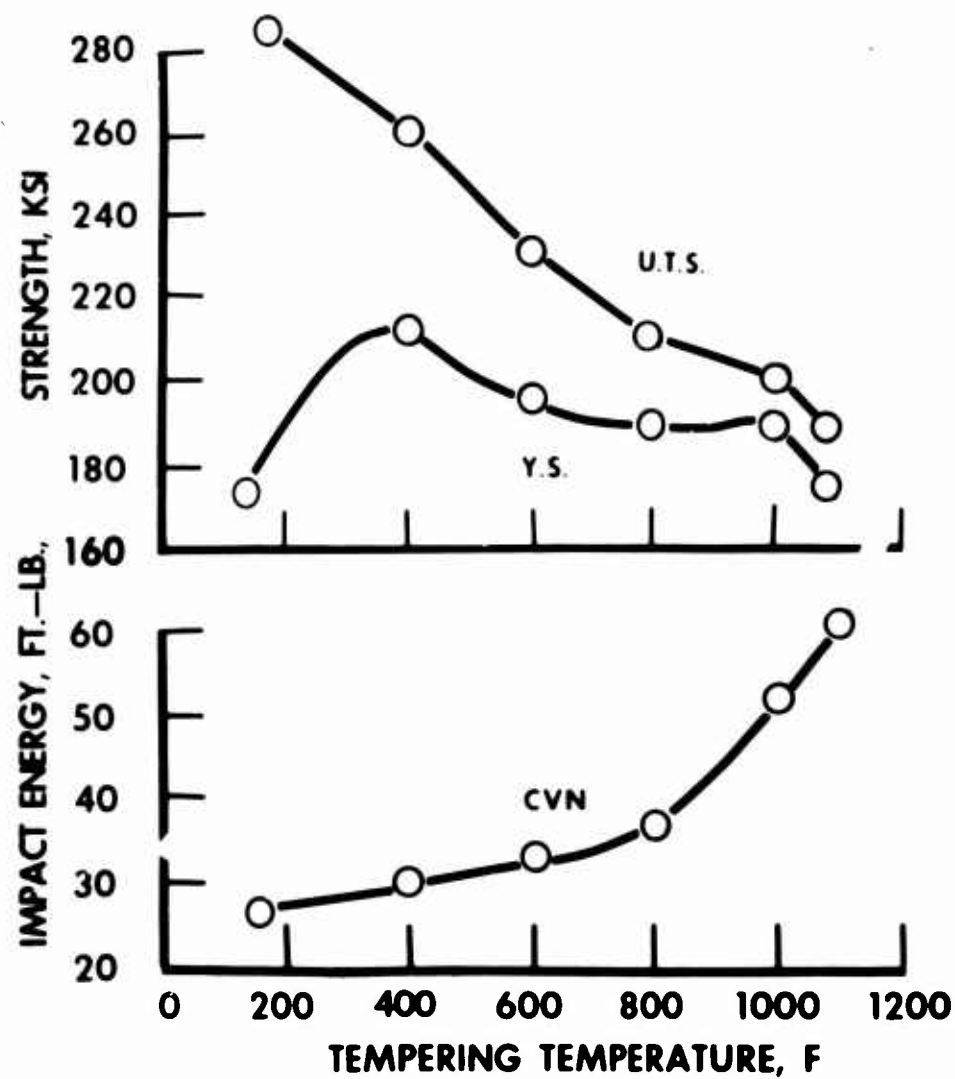


Figure 21. Effect of Tempering Temperature on the Strength and Toughness of HP-9-4-25 Steel. (Reference 31)

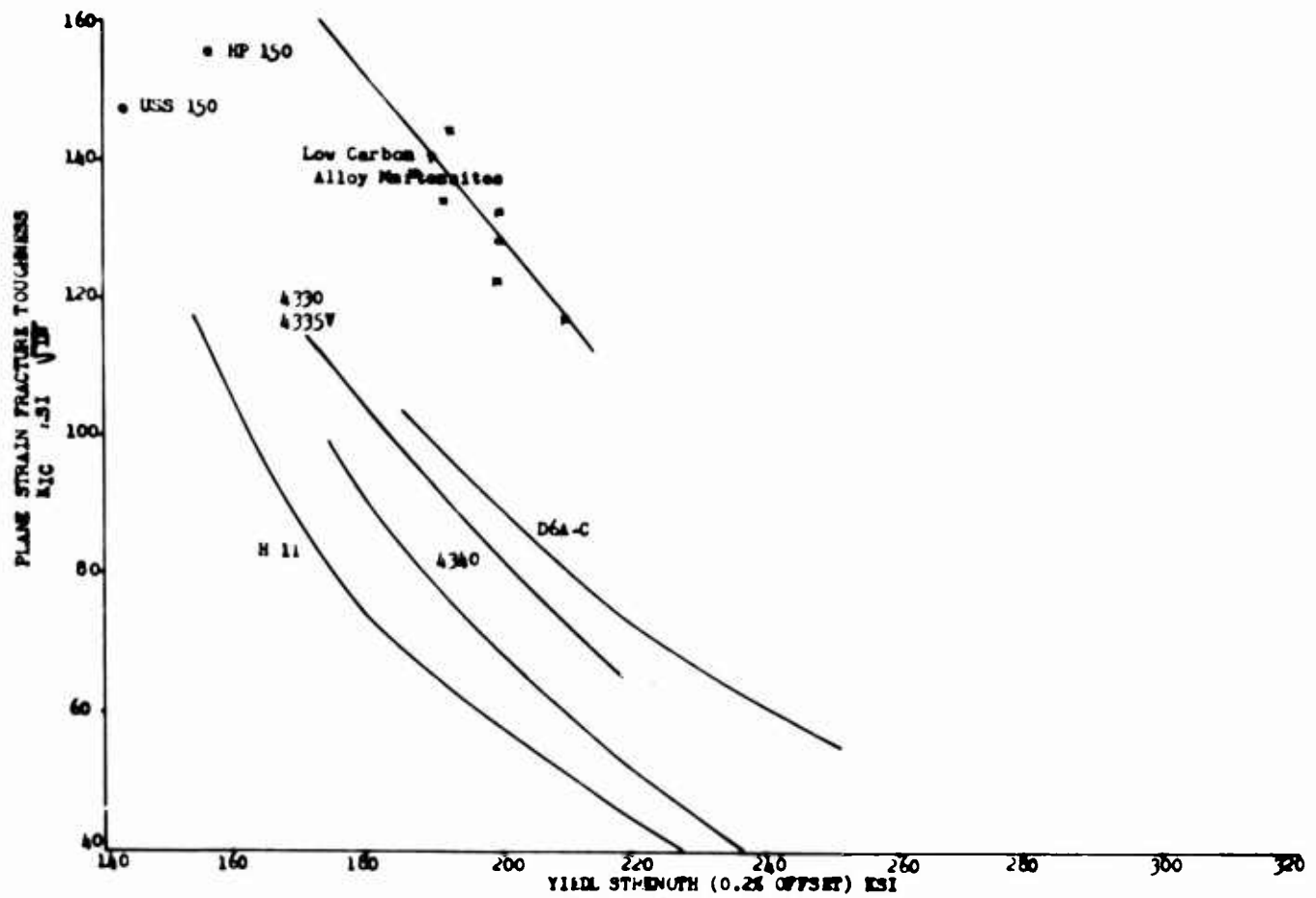


Figure 22. Average Plane Strain Fracture Toughness ( $K_{IC}$ ) Values for Group I and Group II Steels

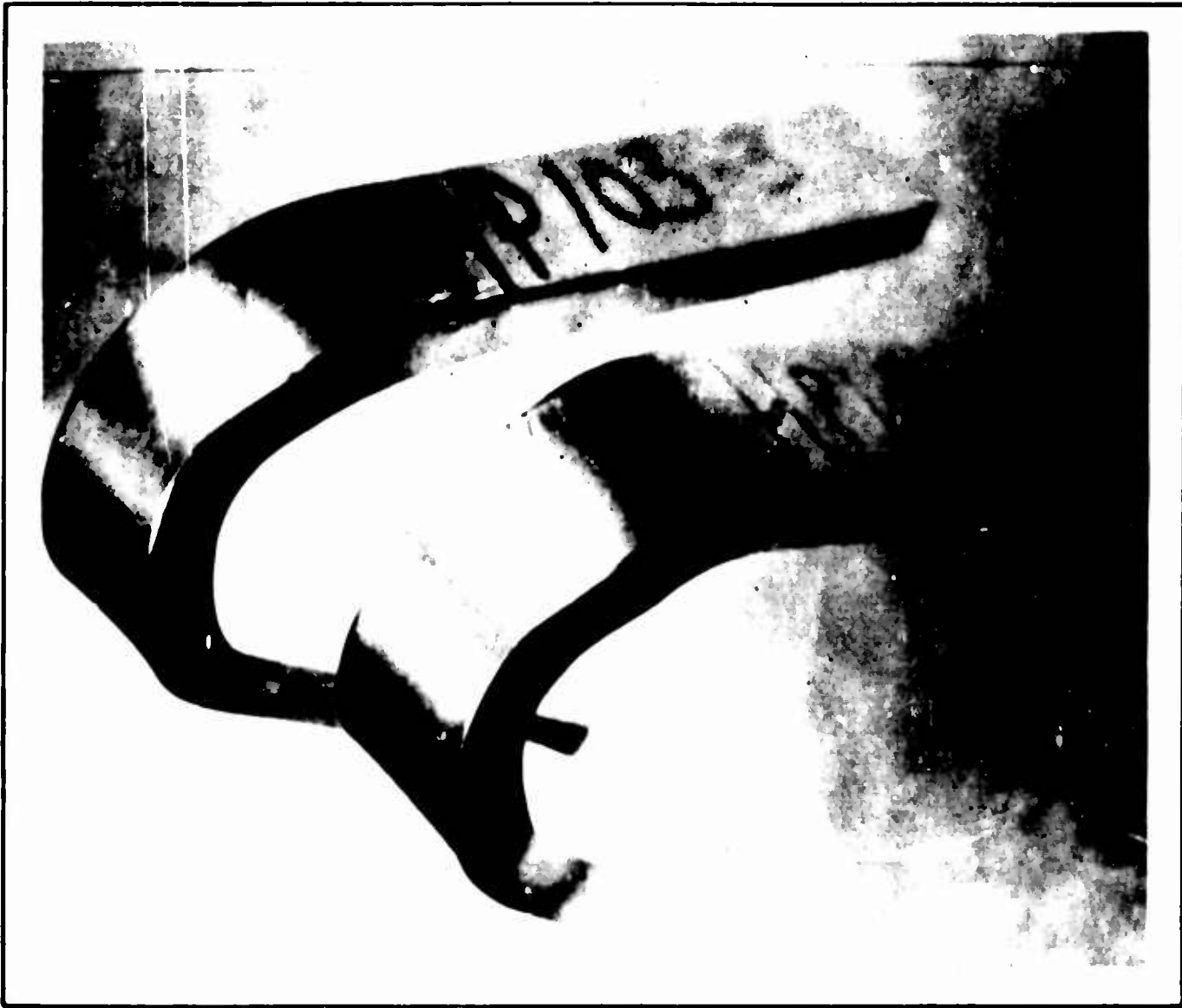


Figure 23. Bend Tests  $\frac{3}{8}$  in. Thick x 1 in. Showing Full Cold Bend Developed With No Evidence of Cracking (Courtesy of Republic Steel Corporation).



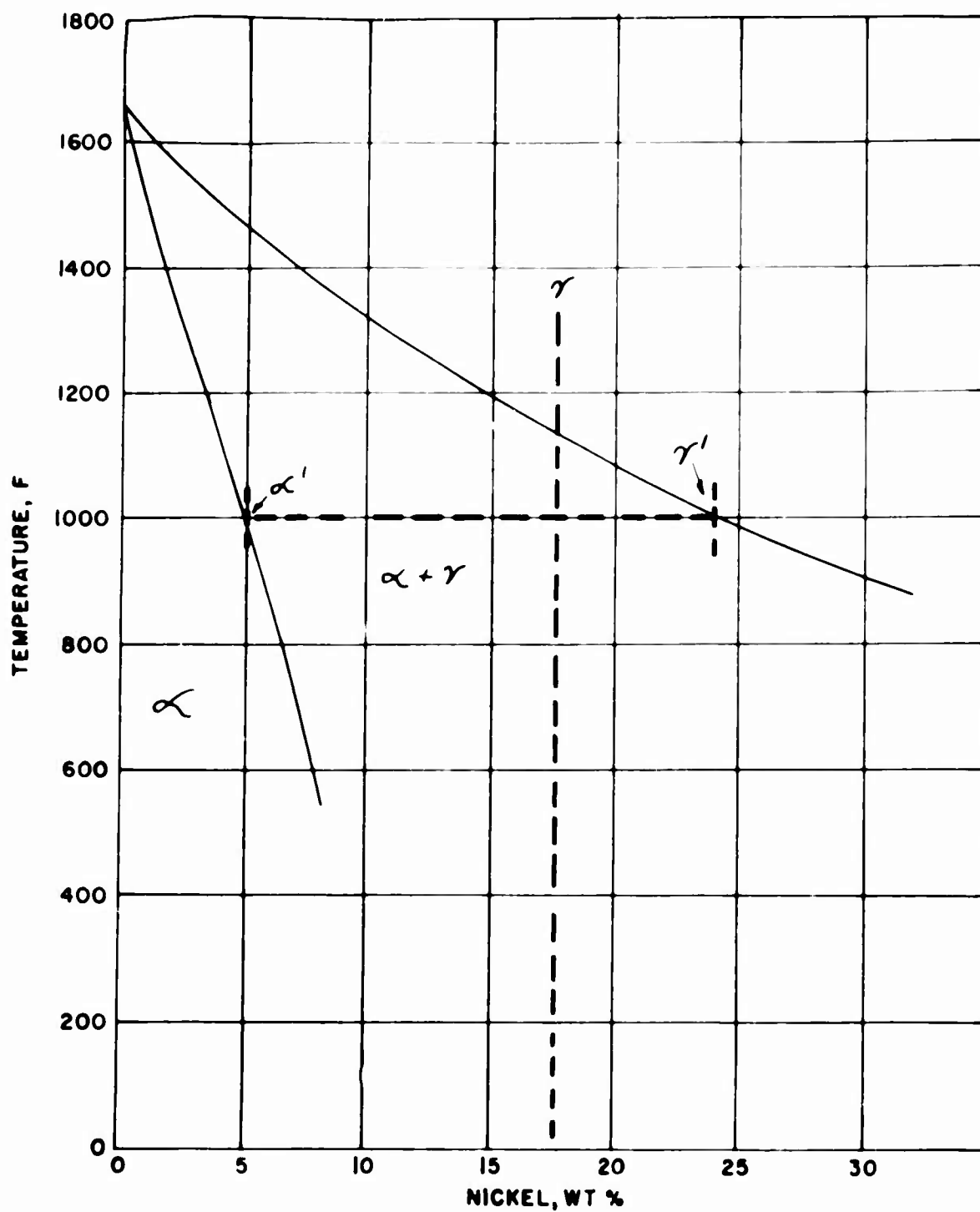


Figure 24. Iron-Nickel Equilibrium Diagram

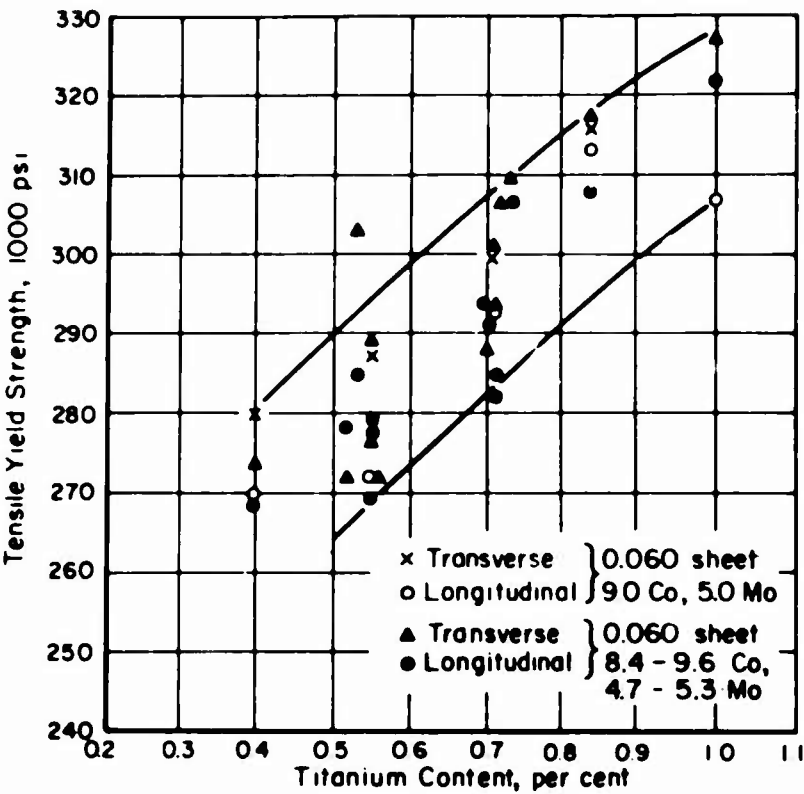


Figure 25. Effect of Titanium Content on the Yield Strength of 18 Ni (300) Maraging Steel Annealed at 1500°F and Aged at 900°F for 3 Hours.



Figure 26. Representative Microstructure of 18% Ni-Co-Mo (270 ksi) 0.400" Plate Etchant: 50 ml HCl + 25 ml HNO<sub>3</sub> - 1 Cu Cl<sub>2</sub> - 15 ml H<sub>2</sub>O Magnification 500X

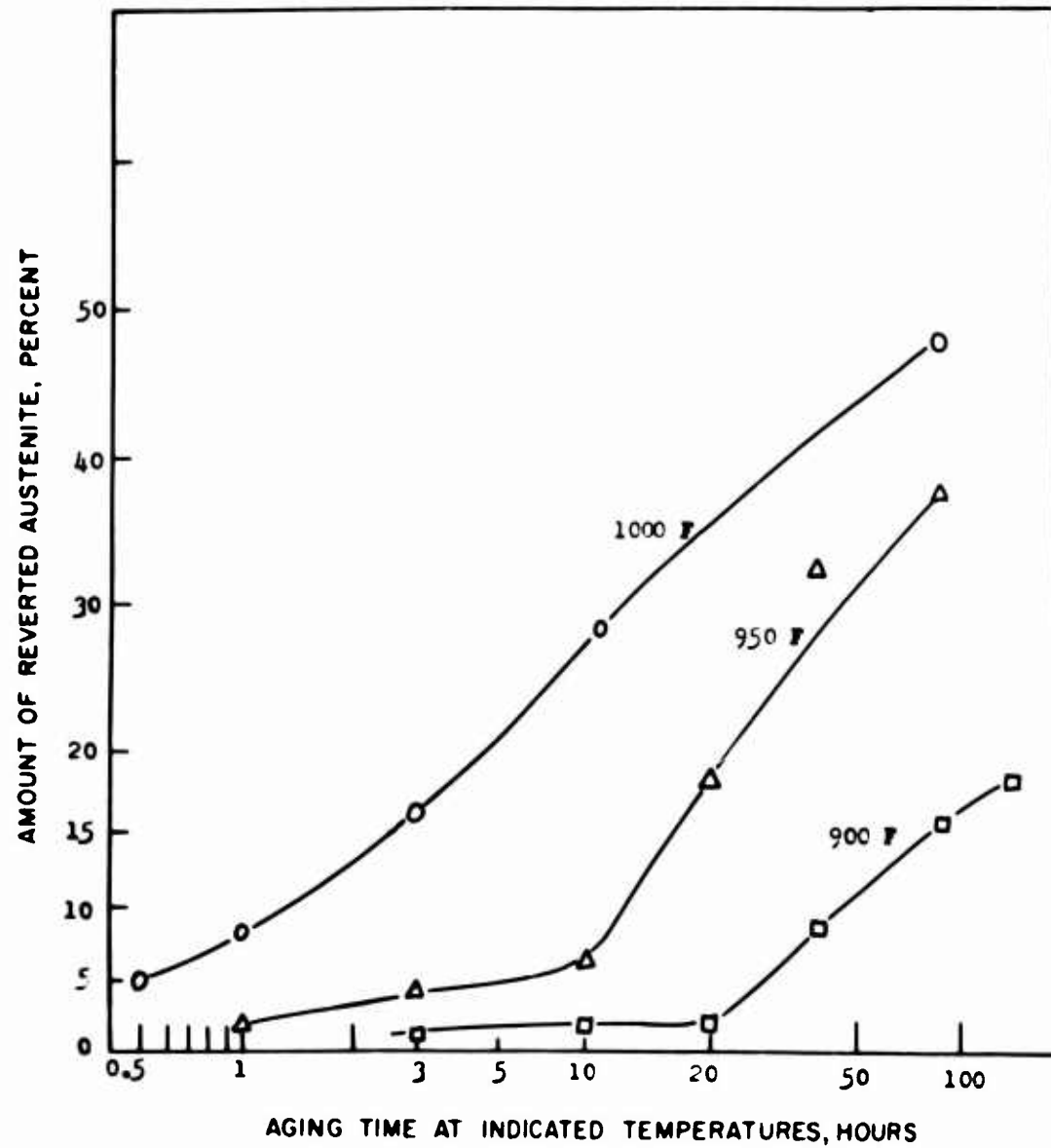
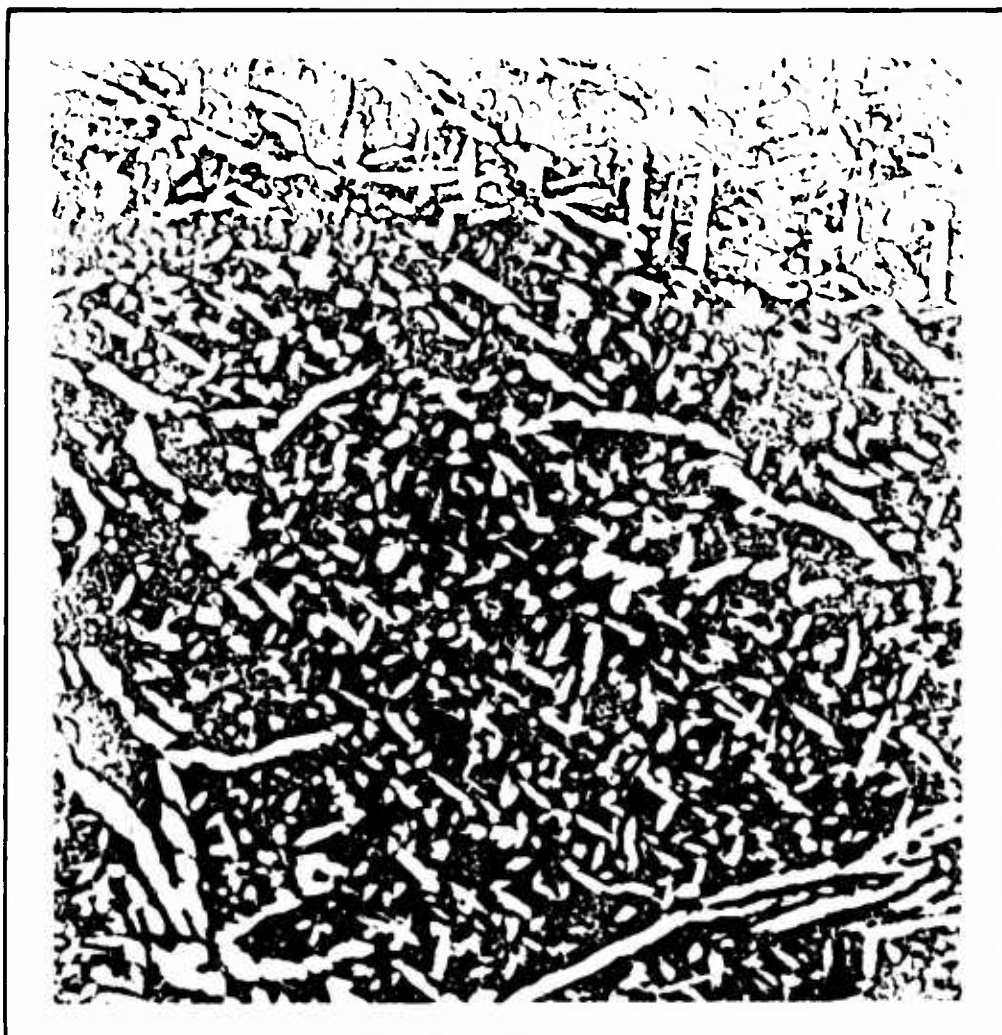


Figure 27A. Amount of Reverted Austenite in Maraging (250) Steel vs Aging Time at Various Temperatures.



**Figure 27B. Electron Micrograph of Surface Replica of 18 Ni (250) Maraging Steel  
Over aged 10 hours at 1000°F.**

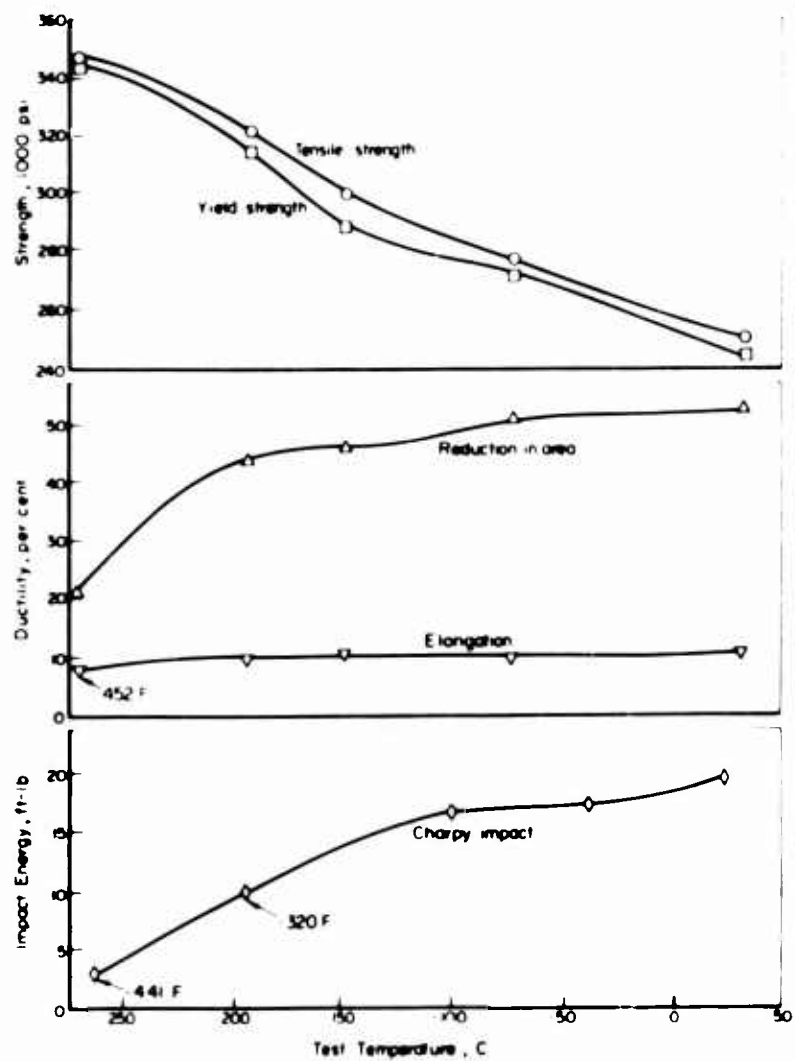


Figure 28. Tensile and Impact Properties of 18 Ni (250) Maraging Steel Plate at Cryogenic Temperatures 1/2 inch Plate

Composition 0.02C, 0.09Si, 0.07Mn, 0.009S, 0.004P, 18.39Ni,  
7.83Co, 4.82Mo, 0.07Al, 0.35Ti.

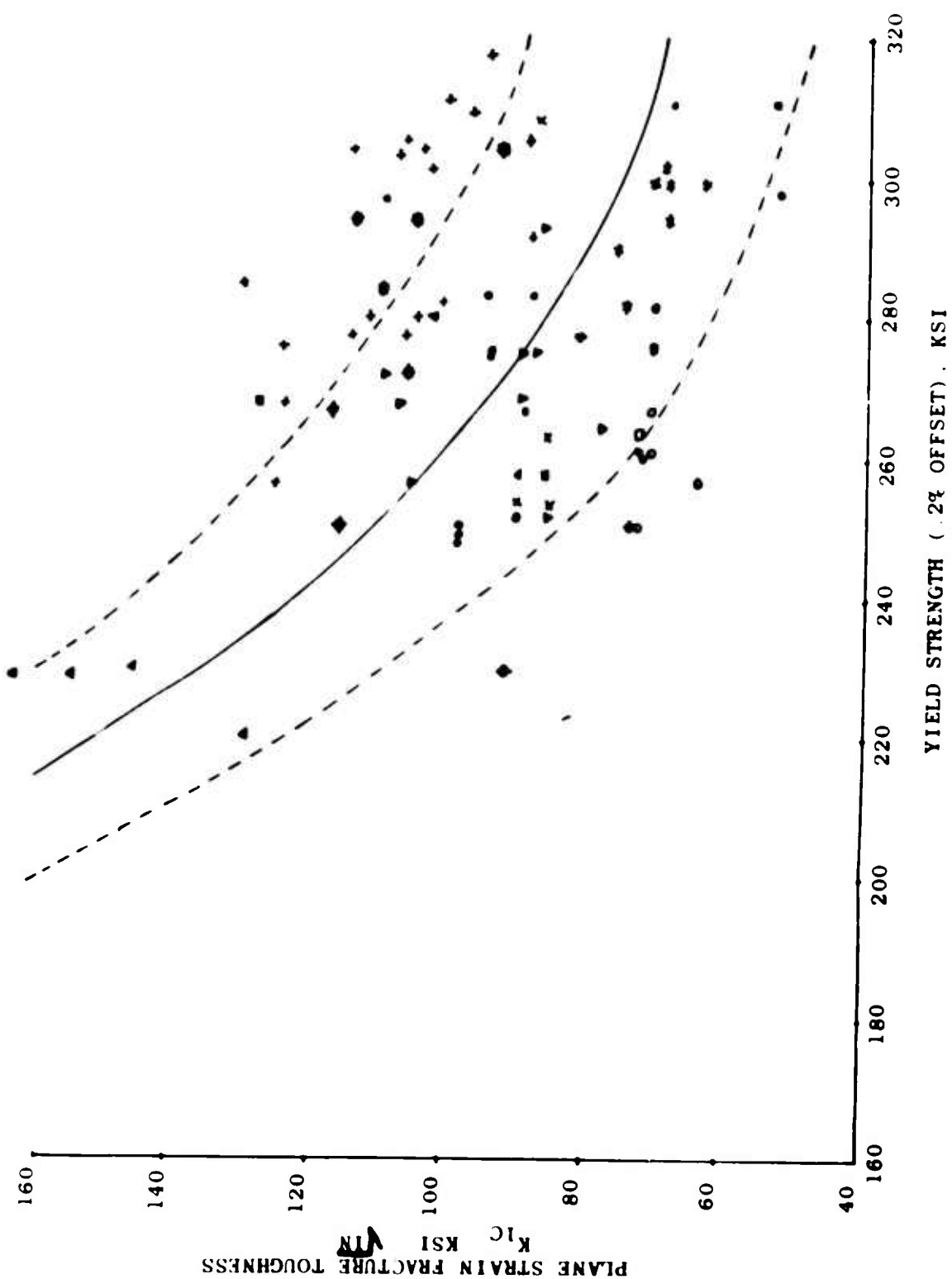


Figure 29. Range of Plane Strain Fracture Toughness Values,  $K_{IC}$ , For 18 Ni Maraging Steels (References 21, 22, 23, 25, 26 and 27)

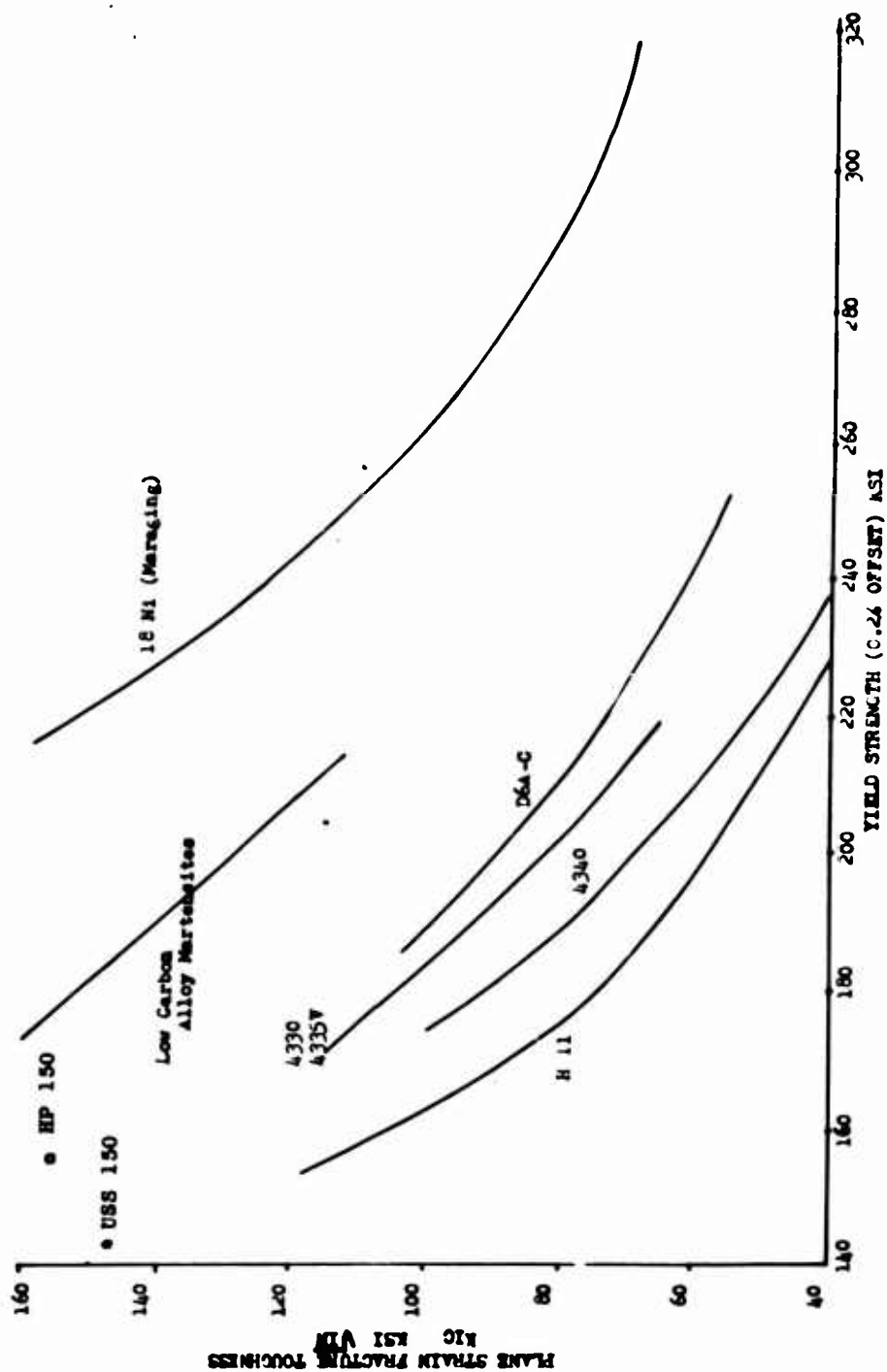


Figure 30. Average Fracture Toughness ( $K_{IC}$ ) Values Versus Yield Strength (Room Temperature) for Groups I, II and III Steels.

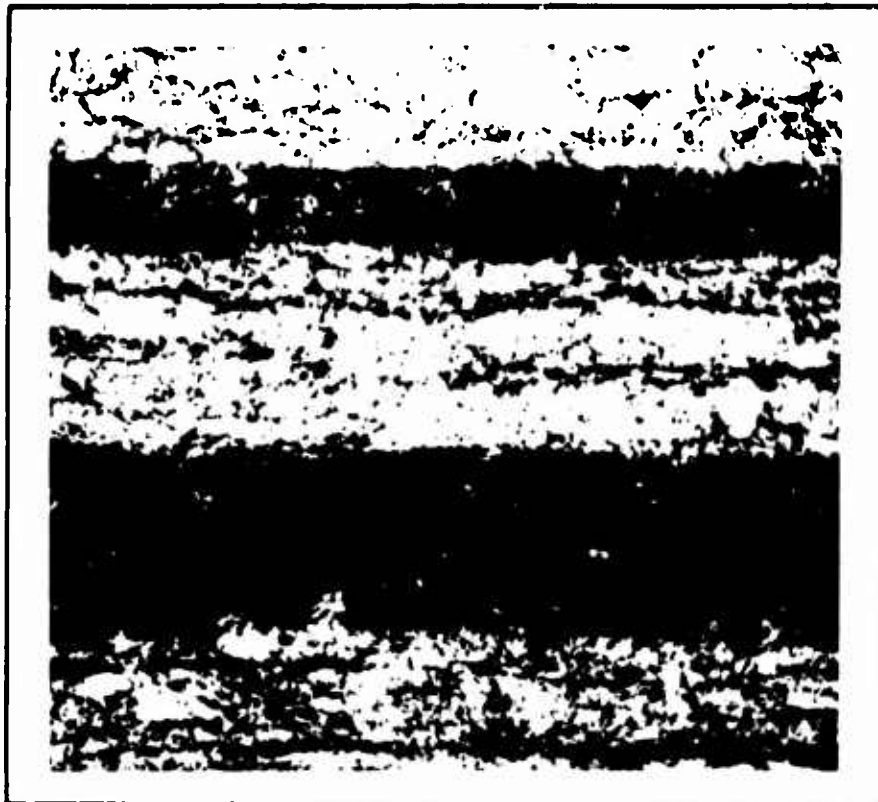


Figure 31. Segregation Observed in 18% Ni-Co Mo (270 ksi) 0.400" Plate. Magnification 500X

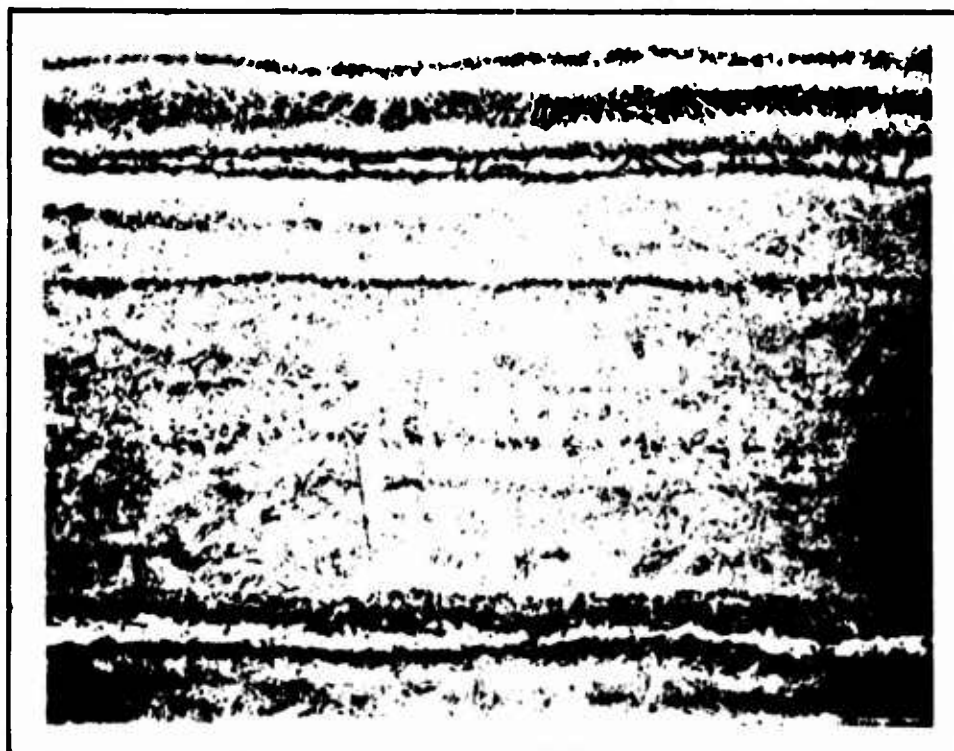


Figure 32. Austenite and Segregation Bands in Rolled Plate of Maraging (250) Steel. Light Micrograph of Polished and Etched Longitudinal Section. X200.





Figure 33A. Fracture Appearance of Smooth and Notched Tension Test Specimens of Maraging (250) Steel Showing Longitudinal "Splits" and "Internal Shear Lips"



Figure 33B. Fracture Path Through Austenite Bands of Test Fracture Shown in A X200

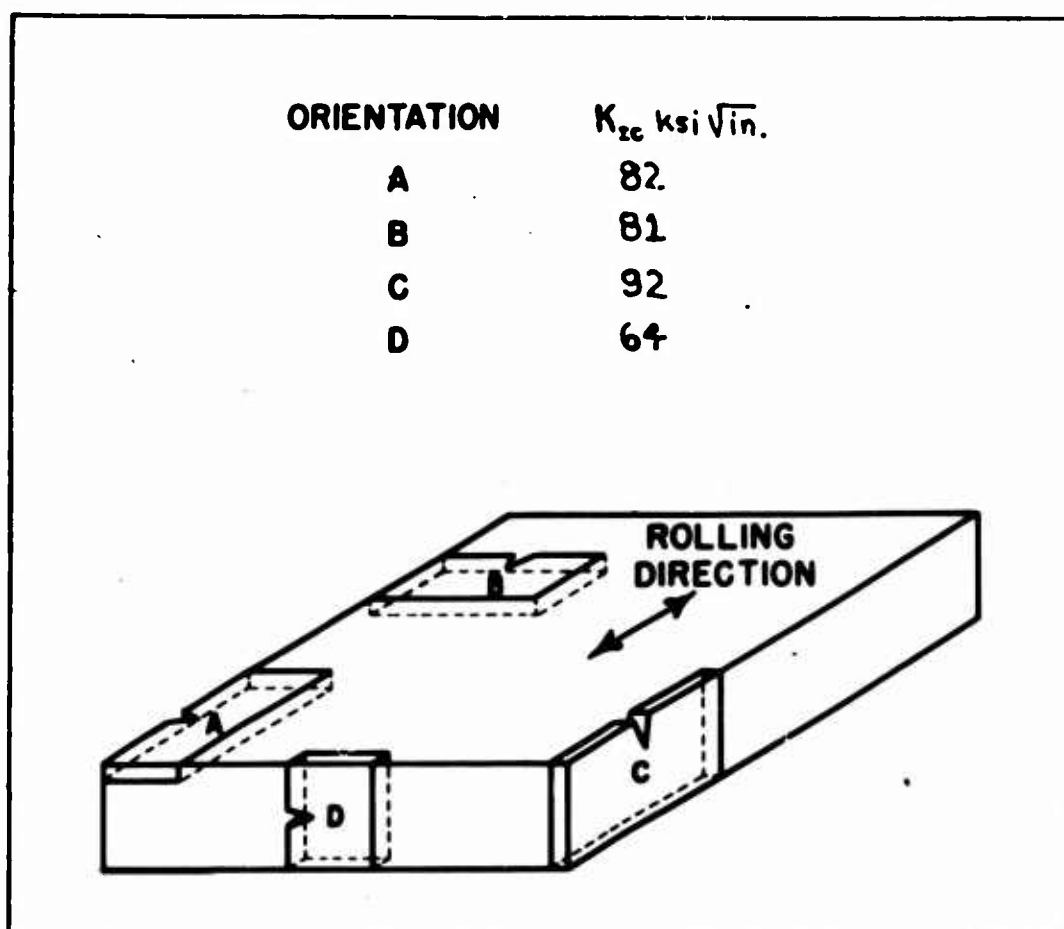


Figure 34. Orientations of Fracture Toughness Specimens Cut from 1 inch thick Plate of Maraging (250) Steel

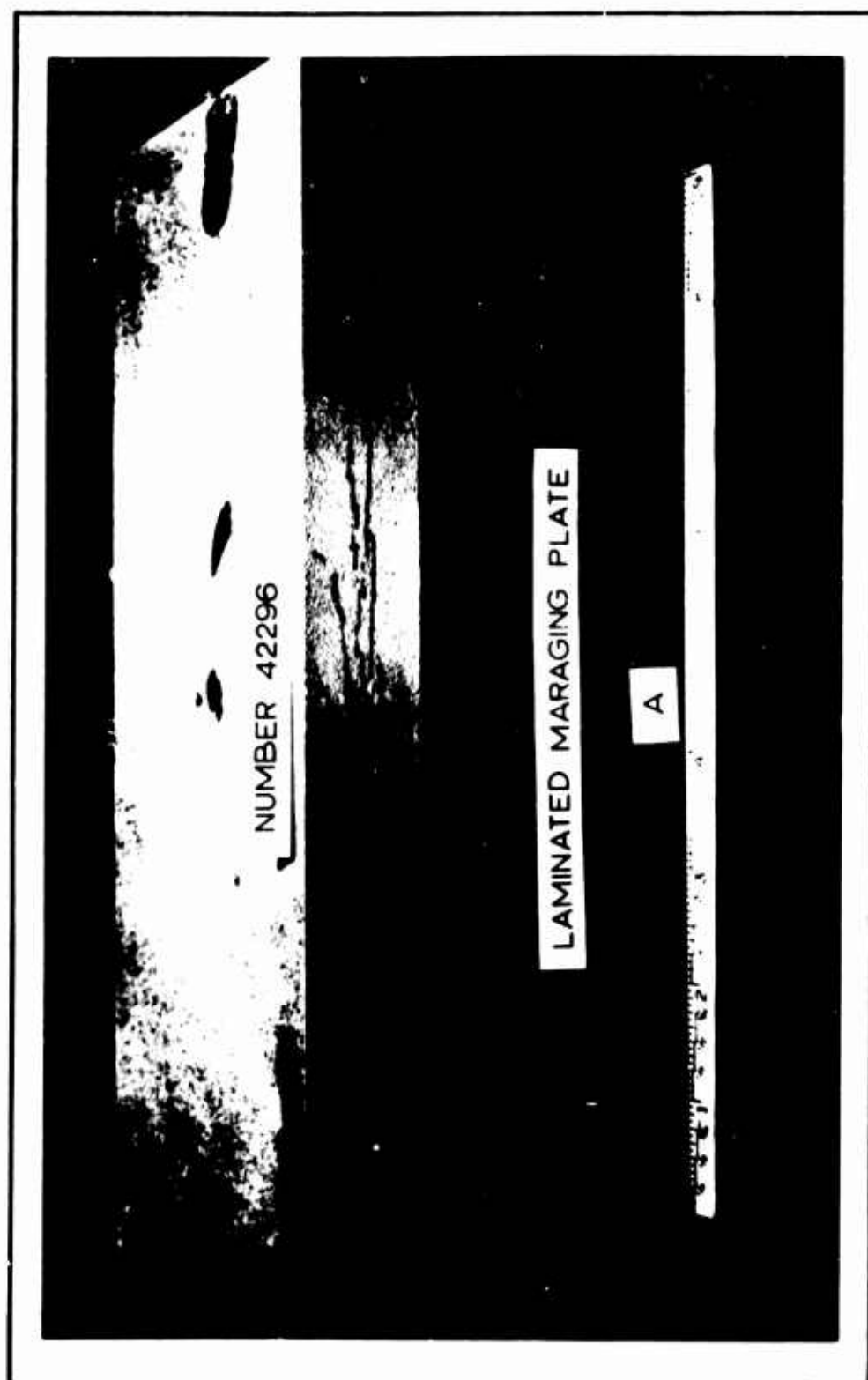


Figure 35. Laminated Maraging Plate

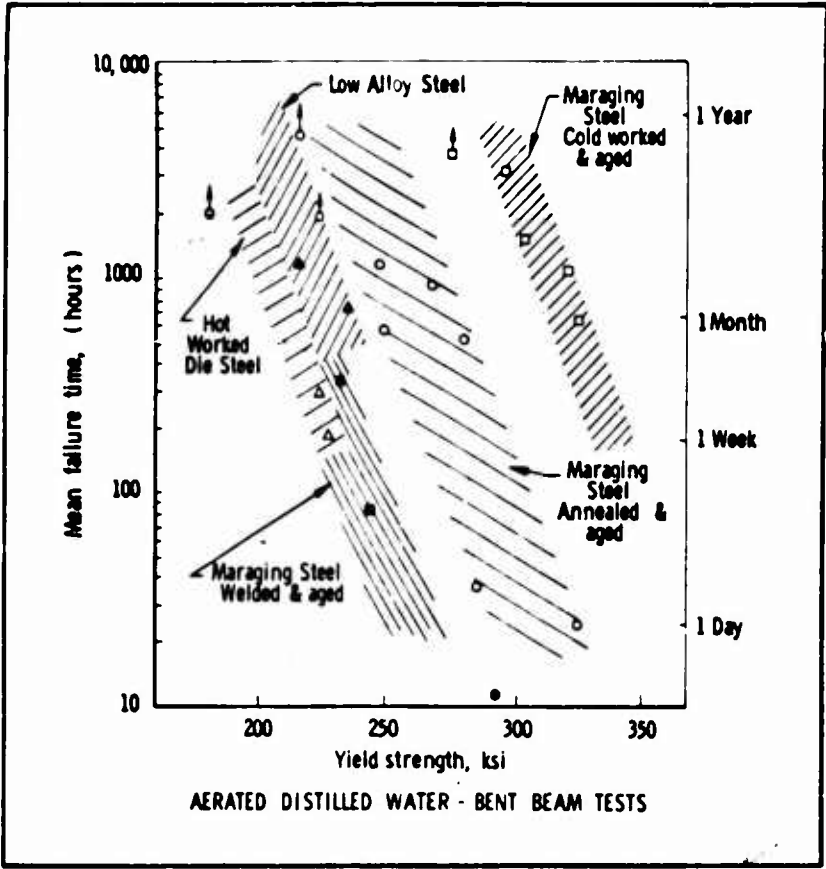


Figure 36. Stress Corrosion Curve

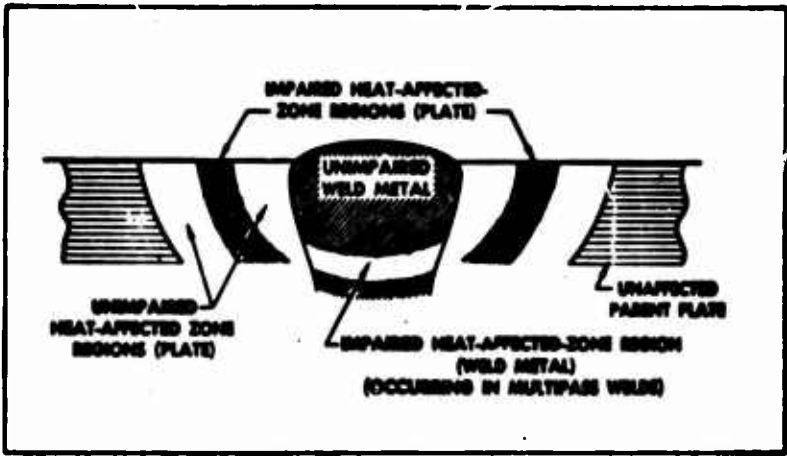


Figure 37. Schematic Illustration of the Different Hardening - Response Regions in 18% Nickel Maraging Steel Weldments

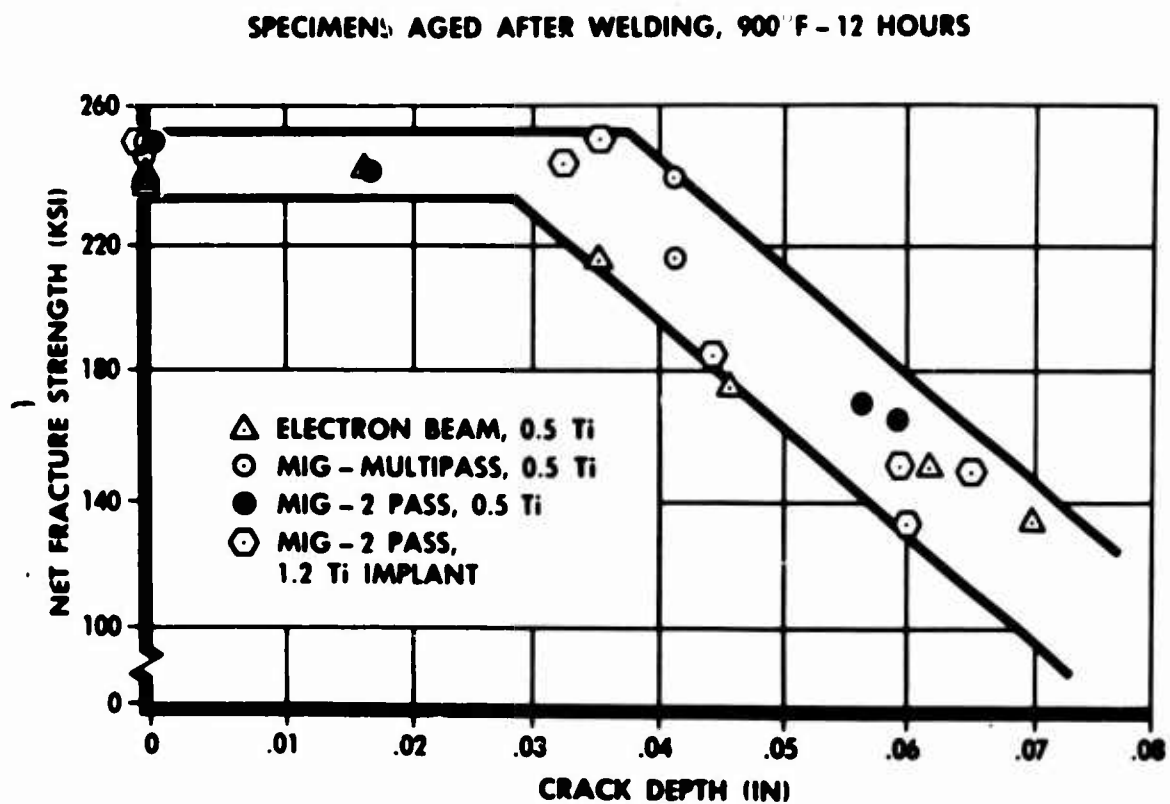


Figure 38. Effect of Weldmetal Composition and Deposition Technique on the Net Fracture Strength in 3/4" 18Ni-7Co-5Mo Airmelted Steel

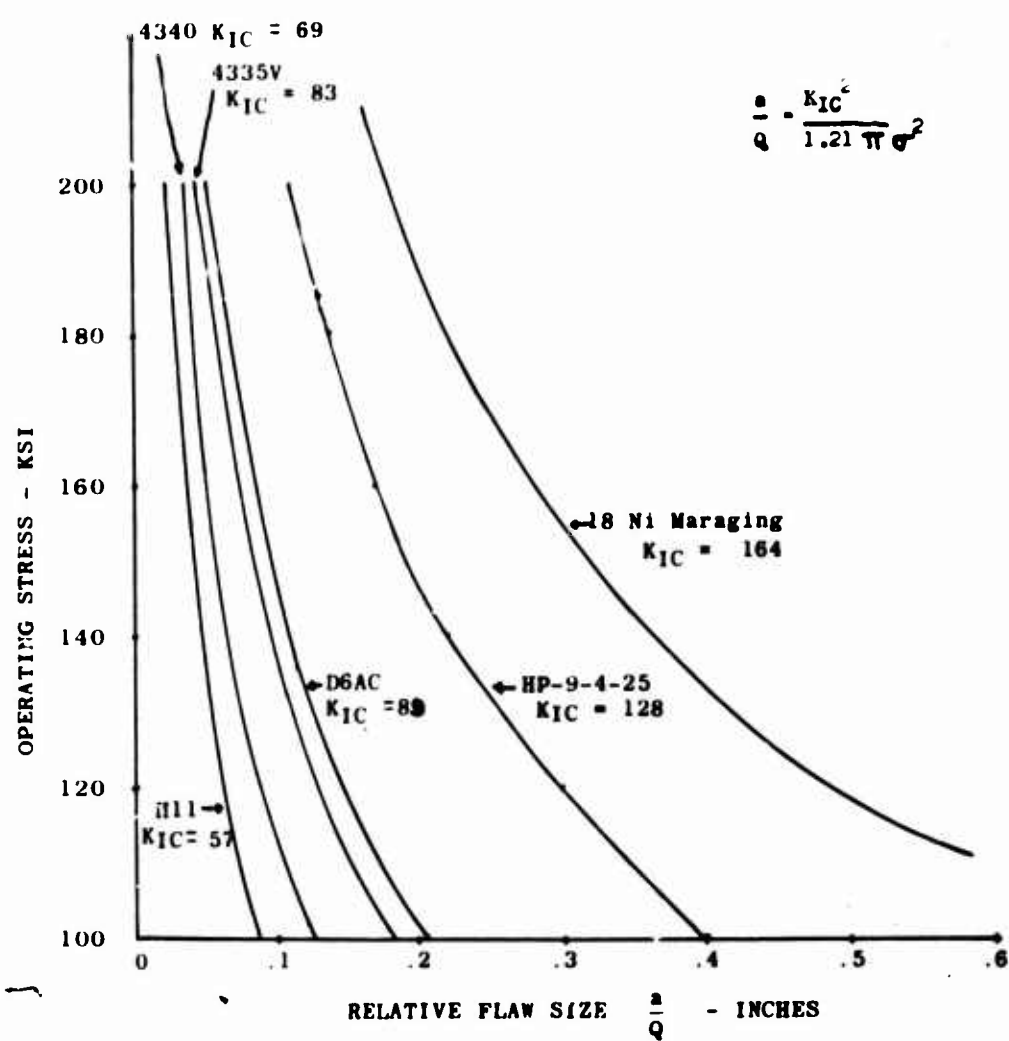


Figure 39. Relative Flaw Sizes of Steels with 200 ksi Yield Strength (.2% Offset)

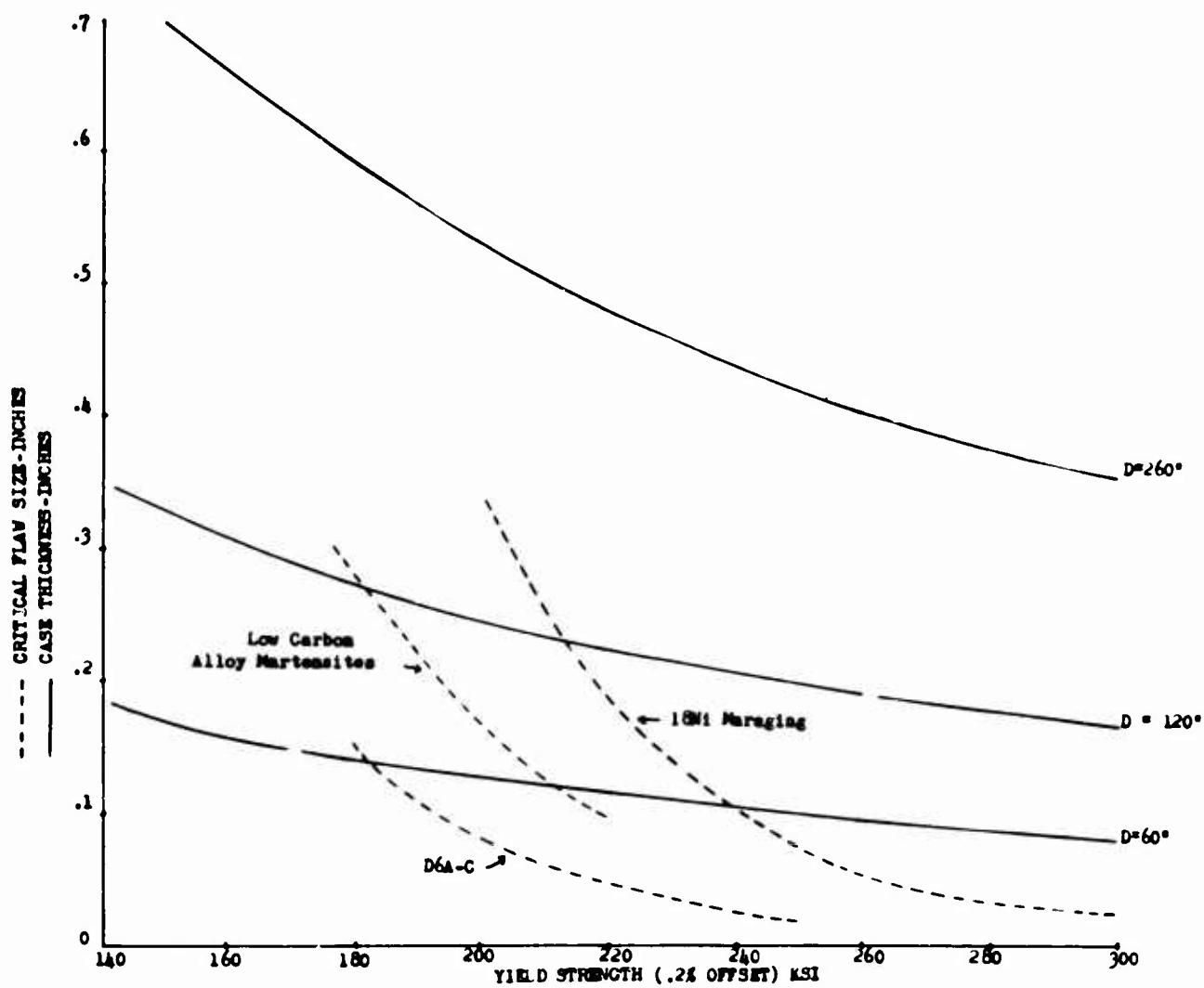


Figure 40. Critical Flaw Size and Case Thickness Versus Yield Strength for Missiles (Internal Pressure = 660 psi)

TABLE 1

## CHEMICAL COMPOSITIONS OF STEELS

Group I - Medium Carbon (.35-.45% Carbon) Low Alloy Martensitic Steels											
Alloy	C%	Mn%	Si%	Ni%	Cr%	Mo%	V%	Co%	Cb%	Ti	Al%
H11	.40	.30	.90	--	5.00	1.30	.50	-	-	-	-
4340	.40	.70	.25	1.80	0.80	.25	-	-	-	-	-
4335V	.36	.70	.27	1.80	0.80	.35	.20	-	-	-	-
4330	.35	.90	1.30	1.80	0.95	.40	.14	-	-	-	-
D6A-C	.45	.80	.25	.50	1.10	1.00	.10	-	-	-	-
Group II - Low Carbon (less than .30% carbon) Alloy Martensites											
USS 150	.10	1.00	.10 max	5.0	1.0	1.0	-	1.0	-	-	-
HP 150	.23/.28	.20 max	.10 max	2.75/3.25	1.40/1.65	.80/1.0	-	-	.03/.07	-	-
9-4-25	.28	.35	.10	8.00	.50	.50	.10	4.00	-	-	-
Group III - 18 Nickel Maraging Steels											
Grade 200	.03 max	.10 max	.10 max	17-19	-	3.0-3.5	-	8.0-9.0	-	0.17-0.25	0.05-0.15
Grade 250	.03 max	.10 max	.10 max	17-19	-	4.6-5.2	-	7.0-8.5	-	0.3-0.5	0.05-0.15
Grade 300	.03 max	.10 max	.10 max	18-19	-	4.6-5.2	-	8.5-9.5	-	0.5-0.8	0.05-0.15

P and S .010% maximum in all steels.



TABLE 2  
MECHANICAL PROPERTIES OF GROUP II LOW CARBON ALLOY MARTENSITES

Alloy	Yield Strength ksi	Tensile Strength ksi	Elongation in 2" %	Reduction in Area %	Room Temperature Impact Strength Charpy V-Notch ft - lb	Reference
USS 150	Base 143 Weld 140	147 148	26 25	64 62	-- --	25
HP 150	Base 157 Weld 172	171 191	20 13	69 --	94 52 (0°F)	16
HP9-4-25	Base 192 Weld 172	201 202	15 13	55 45	50 41	15
HP-9-4-25	Base 196 Weld 198	207 213	15 8	54 51	45 25	15

TABLE 3

PROPERTIES OF TUNGSTEN-INERT-GAS (TIG) ARC WELDED 1 in. HP 9 Ni-4Co . 25C  
 PLATE USING .062 in. dia. FILLER WIRE OF SIMILAR COMPOSITION  
 WITH PLATE IN HEAT TREATED CONDITION

Tensile Data (0.505 in. dia. x 2 in. gage Base Plate Tensile Tests)

<u>Weldment</u>	<u>YS</u> <u>ksi</u>	<u>UTS</u> <u>ksi</u>	<u>RA</u> <u>%</u>	<u>Elong. %</u> <u>in 2 in.</u>
No. 76	193.0	202.3	54.8	14.0
No. 78	189.4	201.0	56.0	15.0
No. 79	192.0	201.0	56.1	16.0

Full Section Transverse Weld Tensiles (.970 in. x .375 in. x 2 in. ga. length)

No. 76	170.0	200.8	40.2	13.0
No. 78	171.6	203.8	46.3	15.0
No. 79	173.5	200.0	47.8	11.0

Transverse Weld Tensile (0.505 in. dia. x 2 in. ga. length)

No. 76	172.6	204.5	52.4	13.0
No. 79	187	202.0	61.1	15.0

Charpy Impact Data (Ft-lbs)

	<u>Weld No. 76</u>		<u>Weld No. 78</u>		<u>Weld No. 79</u>	
	<u>+70F</u>	<u>-80F</u>	<u>+70F</u>	<u>-80F</u>	<u>+70F</u>	<u>-80F</u>
Base Metal	53	43	51	42	46	43, 46
Weld Metal	37	31	41	37	46	33

Plane Strain Fracture Tests

	<u>Pre-Crack Depth (inches)</u>	<u>K<sub>IC</sub></u>	<u>ksi</u>	<u>√in.</u>
HP 76 Weld	.251		119	
HP 76 Base	.228		144	
HP 78 Weld	.282		117	
HP 78 Weld	.237		138	
HP 79 Weld	.239		119	
HP 79 Base	.240		136	

TABLE 4

## CHEMICAL COMPOSITION - 200, 250 and 300 KSI

## 18 PERCENT NICKEL MARAGING STEELS

<u>Element</u>	<u>Grade 200 percent</u>	<u>Grade 250 percent</u>	<u>Grade 300 percent</u>
Carbon	.03 Max.	.03 Max.	.03 Max.
Manganese	.10 Max.	.10 Max.	.10 Max.
Silicon	.10 Max.	.10 Max.	.10 Max.
Phosphorus	.01 Max.	.01 Max.	.01 Max.
Sulfur	.01 Max.	.01 Max.	.01 Max.
Nickel	17-19	17-19	18-19
Titanium	0.15-0.25	0.3-0.5	0.5-0.8
Aluminum	0.05-0.15	0.05-0.15	0.05-0.15
Cobalt	8.0-9.0	7.0-8.5	8.5-9.5
Molybdenum	3.0-3.5	4.6-5.2	4.6-5.2

Other Elements added (percent): 0.003B, 0.002 Zr and 0.05 Ca.

## AVERAGE TENSILE PROPERTIES OF THE

## 18 PERCENT Ni MARAGING STEELS

(Solution Annealed 1500°F - 1 hr, Aged 900°F - 3 to 4 hours)

<u>Property</u>	<u>Grade 200</u>	<u>Grade 250</u>	<u>Grade 300</u>
Tensile Strength (ksi)	L 220-240 T 215-240	255-270 260-273	280-298 278-302
Yield Strength (ksi) (0.2% Offset)	L 215-235 T 210-232	250-260 250-270	275-280 270-285
Elongation %	L 10-13 T 8-11	6-12 5-11.5	3.0-11 4.5-10.5

L and T designate longitudinal and transverse test specimens, respectively.

TABLE 5

PROPERTIES OF WELDS IN 18 PERCENT Ni MARAGING STEEL (Reference 33)

	Gas, Metal Arc (a)		Covered Electrode (b)		Submerged Arc (c)	
	As Welded	Maraged	As Welded	Maraged	As Welded	Maraged
Yield strength (0.2% offset), psi	134,000	220,000	130,000	225,000	130,000	220,000
Tensile strength, psi	154,000	235,000	160,000	242,000	155,000	235,000
Reduction in area, %	40	30	35	26	24	25
Elongation in 1 in., %	5	7	5	6	6	6
Notched: unnotched tensile strength	--	1.2	--	1.1	--	1.1
Rockwell C hardness	32 to 42	49 to 51	30 to 40	49 to 51	30 to 35	48 to 50
Charpy V-notch impact (70 F) (d)	39 ft-lb	15 ft-lb(e)	25 ft-lb	10 ft-lb	33 ft-lb	10 ft-lb

1/2-in. thick plate (250,000 psi yield strength) welded in maraged condition. Transverse tensile tests; all fractures occurred in weld. Maraging was carried out at 900°F for 3 hr.

(a) Semi-automatic, using 0.062-in. diameter filler wire; (b) Low hydrogen flux coating, manual weld; (c) Four passes, welded from one side; (d) Notch in weld running normal to plate surface; (e) 12 ft-lb at -320°F.

TABLE 6  
CRITICAL FLAW SIZES AND CASE THICKNESSES  
FOR  
60-, 120- and 260- IN. DIAMETER STEEL MISSILES  
(Proof Stress =  $\frac{.9}{1.1} F_{TY}$  ; Q = 1)

<u>Case Diameter</u>			
60 inches		120 inches	260 inches
<u>Steel at 200 ksi Yield Strength Level</u>			
Case Thickness, In.	.125	.245	.530
<u>Critical Flaw Size, In.</u>			
D6A-C	.08	.08	.08
HP-9-4-25	.16	.16	.16
18% Ni Maraging	.34	.34	.34
<u>Steel at 250 ksi Yield Strength Level</u>			
Case Thickness, In.	.098	.198	.415
<u>Critical Flaw Sizes, In.</u>			
D6A-C	.02	.02	.02
HP-9-4-25			
18% Ni Maraging	.07	.07	.07

TABLE 7

## MECHANICAL PROPERTIES OF WELDMENTS

Alloy	$K_{IC}$ Toughness (ksi $\sqrt{\text{in.}}$ )	Crack Tolerance (1) Depth (in.)	Yield Strength ksi	Tensile Strength ksi	Elonga- tion % in 1 in.	Redu- tion in Area %
USS 150	Base 147	.42	143	147	44	64
AM <sup>(3)</sup>	Weld 130	.39	140	148	42	62
HP 150	Base 155	.39	157	171	24	66
VM <sup>(4)</sup>	Weld 142	.26	172	191	13	--
4335V	Base 91	.12	166	--	--	--
AM <sup>(3)</sup>	Weld 91	.12	166 <sup>2</sup>	--	--	--
HP 9Ni+4Co+ .25C	Base 139	.21	192	201	15	56
VM <sup>(4)</sup>	Weld 119	.19	172	202	13	45
D6A-C(200)	Base 90	.08	198	213	14	48
AM <sup>(3)</sup>	Weld 74	.06	190	199	--	--
18Ni(200)	Base 164	.24	211	220	--	--
VM <sup>(4)</sup>	Weld 131	.15	210	213	--	--
18Ni(250)	Base 88	.05	257	270	8	37
VM <sup>(4)</sup>	Weld 55	.02	239	252	3	4

(1) Depth of surface crack with length =  $7.15 \times \text{depth}$  (or  $Q = 1$ ). This is sufficient to cause fracture at operating stress equal to  $\frac{.9}{1.1} F_{ty} = .82$  yield strength.

(2) Yield strength of weld assumed equal to base metal.

(3) Air Melted

(4) Vacuum Melted

## APPENDIX

## STRUCTURAL-WEIGHT MATERIAL INDEXES

Since the propellant can be assumed to occupy a given volume, it is convenient to evaluate motor-case materials on the basis of the  $W/V$  ratio where  $W$  = material weight of the cylindrical portion of the case and  $V$  = volume enclosed by this portion. Since  $W \approx \pi D t d$  and  $V \approx \pi D^2$  for unit length of cylinder,

$$\frac{W}{V} = \frac{4td}{D} \quad (3)$$

where  $W$  = weight of unit length of cylinder  
 $V$  = enclosed volume of unit length of cylinder  
 $t$  = motor-case thickness  
 $d$  = case material density  
 $D$  = mean diameter of motor-case.

For any given material and case diameter, the  $W/V$  ratio is directly related to the thickness ( $t$ ) and therefore minimum-weight design is governed by the minimum thickness required to withstand the critical design stresses.

## Internal Pressure

The largest stress,  $S$ , (hoop stress) in a motor-case subjected to internal pressure is given by

$$S = \frac{kpD}{2t} \quad (4)$$

where  $k$  is a factor depending on end closure design,  $p$  is the internal pressure, and  $D$  and  $t$  are the mean diameter and wall thickness of the motor case. Substitution of the thickness value from Equation 4 in Equation 3 gives a  $W/V$  ratio where internal pressure is critical:

$$\frac{W}{V} = \frac{2kp}{S/d} \quad (5)$$

The calculations for Figure 3 were made with the following assumptions  $k = 1$ ,  $S$  = material tensile strength divided by a safety factor of 1.25 and material properties given in Table 8.

## Buckling and Bending

The critical buckling stress  $(F_c)_{cr}$  for a motor-case in axial compression is given by

$$(F_c)_{cr} = \frac{2CEt}{D} \quad (6)$$

where  $E$  = elastic modulus and  $C$  is a coefficient which depends somewhat on the  $D/t$  ratio and ranges from 0.185 to 0.3 (mean value) (Reference Abraham, L. H. "Structural Design of Missiles and Spacecraft", McGraw-Hill Book Co. Inc., New York, 1962 pages 182-184).

For design,  $F_{(c)cr}$  is the critical axial load,  $P$ , multiplied by a safety factor,  $N$ , and divided by the cross-sectional area ( $\pi Dt$ ) of the case or

$$F_{(c)cr} = \frac{PN}{\pi Dt} \quad (7)$$

Solving Equations 6 and 7 for wall thickness ( $t$ ) and substituting  $t$  in Equation 3 gives

$$\frac{W}{V} = \frac{1}{\sqrt{E}/d} \sqrt{\frac{8PN/D^2}{C}} \quad (8)$$

The requirement that buckling takes place in the elastic range means that  $F_{(c)cr}$  where  $N = 1$  cannot exceed the material compressive yield strength. This imposes the following upper limit on the axial load,  $P$ :

$$\frac{P_{max.}}{D^2} = \frac{\pi}{2C} \frac{F_{cy}^2}{E} \quad (9)$$

For values of  $F_{cy}^2/E$  all materials currently under consideration and for current and contemplated external loads on motor-cases, Equation 9 will not be a limitation. Therefore, the structural weight material index of minimum-weight design for external loads is  $\sqrt{E}/d$  in Equation 8.

When both compressive and bending loads are acting, Abraham (above reference) gives interaction equation as

$$\frac{F_c}{(F_c)_{cr}} + \frac{F_B}{(F_B)_{cr}} = 1 \quad (10)$$

where  $F_c$  and  $F_B$  are the direct compressive and bending stresses,  $(F_c)_{cr}$  is as defined in Equation 6 and  $(F_B)_{cr}$  is the bending stress for buckling under bending alone.

Relationship between  $(F_B)_{cr}$  and  $(F_c)_{cr}$  is given by Abraham as

$$F_B = 1.35 (F_c)_{cr} \quad (11)$$



Bending stresses in a thin-wall cylinder is expressed by

$$F_B = \frac{Mc}{I} = \frac{4M}{\pi D^2 t} \quad (12)$$

where M is the bending moment and  $I/C$  is the section modulus.

Combining Equations 10, 11 and 12, gives the following expression for the equivalent combined loading  $P_{eq}$  as used in Figure 3:

$$P_{eq} = P + \frac{4M}{1.35D} \quad (13)$$

Substitution of  $P_{eq}$  for P in Equation 8 furnishes the equation used for calculations made for Figure 3:

$$\frac{W}{V} = \frac{1}{\sqrt{E}} \sqrt{\frac{8P_{eq} N/D^2}{C}} \quad (14)$$

The following assumptions were made in the calculations:

$$N = 1$$

$$C = 0.3$$

$$P_{eq} \text{ for design} = \frac{P_{eq}}{1.52} \text{ to credit 52 percent increase}$$

in buckling resistance due to a case-bonded propellant. Material properties used are listed in Table 8.

TABLE 8  
MATERIAL PROPERTIES

Material	Minimum Tensile Strength ( $F_{tu}$ ) ksi	Density, $d$ , Pounds per cu in. (psi)	Modulus, E, millions of psi	$F_{tu}/d$ millions of psi/pci	E/d psi pci
X7106 Aluminum Alloy	60	.10	10.3	.60	32,100
7051 T651 Aluminum Alloy	85	.10	10.3	.85	32,100
18 Ni-Co-Mo (200)	200	.29	26.5	.69	17,800
18 Ni-Co-Mo (300)	300	.29	26.5	1.03	17,800
Ti-6 Al-4V	160	.161	16	.995	24,800
Future Ti Alloy	200	.161	16	1.24	24,800
Glass-Resin	94	.072	2.5	1.31	22,000
Glass-Resin	120	.072	2.5	1.67	22,000

Unclassified

Security Classification

DOCUMENT CONTROL DATA - R&D		
(Security classification of title, body of abstract and indexing annotation must be entered when the overall report is classified)		
1 ORIGINATING ACTIVITY (Corporate author) Physical Metallurgy Branch Metals and Ceramics Division Air Force Materials Laboratory		2a REPORT SECURITY CLASSIFICATION Unclassified
		2b GROUP
3 REPORT TITLE Steels for Solid-Propellant Rocket-Motor Cases		
4 DESCRIPTIVE NOTES (Type of report and inclusive dates) Survey of Rocket-Motor Case Materials. July-October 1964.		
5 AUTHOR(S) (Last name, first name, initial) Perlmutter, Isaac and DePierre, Vincent		
6 REPORT DATE January 1965	7a TOTAL NO OF PAGES 78	7b NO OF REFS 37
8a CONTRACT OR GRANT NO	9a ORIGINATOR'S REPORT NUMBER(S) AFML Technical Report 64-356	
b. PROJECT NO 7351		
c.	9b. OTHER REPORT NO(S) (Any other numbers that may be assigned this report)	
d.		
10 AVAILABILITY/LIMITATION NOTICES Releasable to "OTS".		
11 SUPPLEMENTARY NOTES	12 SPONSORING MILITARY ACTIVITY AFML	
13 ABSTRACT On the basis of strength considerations, a comparison of rocket-motor case materials (titanium alloys, aluminum alloys, composite fibre glass and steels) shows that steel would result in the heaviest cases. However the current technology of steel places this material in a much more competitive position to meet the manufacturing technology required for large motor cases (above 120" diameter). Plane strain fracture toughness is used as a parameter of material reliability (performance according to design prediction). The relations between fracture toughness, yield strength, operational stress and geometry of defects and the use of these data in design are discussed. Three groups of steel (martensitic steels, low alloy martensites and maraging steels) are compared on the basis of fracture toughness-yield strength relation and weldability. The latter two groups are the outstanding candidates for application to large cases where processing prior to welding is mandatory. The importance of future alloy steel development in the direction of improved balance between fracture toughness and yield strength for higher reliability is emphasized.		

Unclassified

Security Classification

14 KEY WORDS	LINK A		LINK B		LINK C	
	ROLE	WT	ROLE	WT	ROLE	WT
Rocket-Motor Case Materials Plane Strain Fracture Toughness of Steels Weldability of Steels Low Alloy Medium Carbon Martensitic Steels Low Carbon Alloy Martensites Maraging Steels						

INSTRUCTIONS

1. **ORIGINATING ACTIVITY:** Enter the name and address of the contractor, subcontractor, grantee, Department of Defense activity or other organization (*corporate author*) issuing the report.

2a. **REPORT SECURITY CLASSIFICATION:** Enter the overall security classification of the report. Indicate whether "Restricted Data" is included. Marking is to be in accordance with appropriate security regulations.

2b. **GROUP:** Automatic downgrading is specified in DoD Directive 5200.10 and Armed Forces Industrial Manual. Enter the group number. Also, when applicable, show that optional markings have been used for Group 3 and Group 4 as authorized.

3. **REPORT TITLE:** Enter the complete report title in all capital letters. Titles in all cases should be unclassified. If a meaningful title cannot be selected without classification, show title classification in all capitals in parenthesis immediately following the title.

4. **DESCRIPTIVE NOTES:** If appropriate, enter the type of report, e.g., interim, progress, summary, annual, or final. Give the inclusive dates when a specific reporting period is covered.

5. **AUTHOR(S):** Enter the name(s) of author(s) as shown on or in the report. Enter last name, first name, middle initial. If military, show rank and branch of service. The name of the principal author is an absolute minimum requirement.

6. **REPORT DATE:** Enter the date of the report as day, month, year, or month, year. If more than one date appears on the report, use date of publication.

7a. **TOTAL NUMBER OF PAGES:** The total page count should follow normal pagination procedures, i.e., enter the number of pages containing information.

7b. **NUMBER OF REFERENCES:** Enter the total number of references cited in the report.

8a. **CONTRACT OR GRANT NUMBER:** If appropriate, enter the applicable number of the contract or grant under which the report was written.

8b, 8c, & 8d. **PROJECT NUMBER:** Enter the appropriate military department identification, such as project number, subproject number, system numbers, task number, etc.

9a. **ORIGINATOR'S REPORT NUMBER(S):** Enter the official report number by which the document will be identified and controlled by the originating activity. This number must be unique to this report.

9b. **OTHER REPORT NUMBER(S):** If the report has been assigned any other report numbers (*either by the originator or by the sponsor*), also enter this number(s).

10. **AVAILABILITY/LIMITATION NOTICES:** Enter any limitations on further dissemination of the report, other than those

imposed by security classification, using standard statements such as:

- (1) "Qualified requesters may obtain copies of this report from DDC."
- (2) "Foreign announcement and dissemination of this report by DDC is not authorized."
- (3) "U. S. Government agencies may obtain copies of this report directly from DDC. Other qualified DDC users shall request through \_\_\_\_\_."
- (4) "U. S. military agencies may obtain copies of this report directly from DDC. Other qualified users shall request through \_\_\_\_\_."
- (5) "All distribution of this report is controlled. Qualified DDC users shall request through \_\_\_\_\_."

If the report has been furnished to the Office of Technical Services, Department of Commerce, for sale to the public, indicate this fact and enter the price, if known.

11. **SUPPLEMENTARY NOTES:** Use for additional explanatory notes.

12. **SPONSORING MILITARY ACTIVITY:** Enter the name of the departmental project office or laboratory sponsoring (paying for) the research and development. Include address.

13. **ABSTRACT:** Enter an abstract giving a brief and factual summary of the document indicative of the report, even though it may also appear elsewhere in the body of the technical report. If additional space is required, a continuation sheet shall be attached.

It is highly desirable that the abstract of classified reports be unclassified. Each paragraph of the abstract shall end with an indication of the military security classification of the information in the paragraph, represented as (TS), (S), (C), or (U).

There is no limitation on the length of the abstract. However, the suggested length is from 150 to 225 words.

14. **KEY WORDS:** Key words are technically meaningful terms or short phrases that characterize a report and may be used as index entries for cataloging the report. Key words must be selected so that no security classification is required. Identifiers, such as equipment model designation, trade name, military project code name, geographic location, may be used as key words but will be followed by an indication of technical context. The assignment of links, rules, and weights is optional.

Unclassified

Security Classification